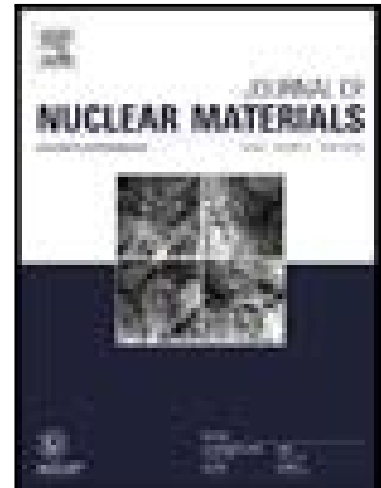


Journal Pre-proof

Effect of hydrogen gas and leaching solution on the fast release of fission products from two PWR fuels



T. Mennecart , L. Iglesias , M. Herm , T. König , G. Leinders ,
C. Cachoir , K. Lemmens , M. Verwerft , V. Metz ,
E. González-Robles , K. Meert , T. Vandoorne , R. Gaggiano

PII: S0022-3115(23)00578-0
DOI: <https://doi.org/10.1016/j.jnucmat.2023.154811>
Reference: NUMA 154811

To appear in: *Journal of Nuclear Materials*

Received date: 7 July 2023
Revised date: 3 September 2023
Accepted date: 1 November 2023

Please cite this article as: T. Mennecart , L. Iglesias , M. Herm , T. König , G. Leinders , C. Cachoir , K. Lemmens , M. Verwerft , V. Metz , E. González-Robles , K. Meert , T. Vandoorne , R. Gaggiano , Effect of hydrogen gas and leaching solution on the fast release of fission products from two PWR fuels, *Journal of Nuclear Materials* (2023), doi: <https://doi.org/10.1016/j.jnucmat.2023.154811>

This is a PDF file of an article that has undergone enhancements after acceptance, such as the addition of a cover page and metadata, and formatting for readability, but it is not yet the definitive version of record. This version will undergo additional copyediting, typesetting and review before it is published in its final form, but we are providing this version to give early visibility of the article. Please note that, during the production process, errors may be discovered which could affect the content, and all legal disclaimers that apply to the journal pertain.

© 2023 Published by Elsevier B.V.

Effect of hydrogen gas and leaching solution on the fast release of fission products from two PWR fuels

T. Mennecart^{1,*}, L. Iglesias², M. Herm², T. König², G. Leinders³, C. Cachoir¹, K. Lemmens¹, M. Verwerft³, V. Metz², E. González-Robles⁴, K. Meert⁵, T. Vandoorne⁵, R. Gaggiano⁵

¹ Institute for Sustainable Waste & Decommissioning, Belgian Nuclear Research Centre, 2400 Mol, Belgium

² Karlsruhe Institute of Technology, Institute for Nuclear Waste Disposal, P.O. Box 3640, 76021 Karlsruhe, Germany

³ Institute for Nuclear Energy Technology, Belgian Nuclear Research Centre, 2400 Mol, Belgium

⁴ Fundació Institut d'Investigació Sanitària Illes Balears, Carretera de Valldemossa, 79, 07120 Palma, Balearic Islands, Spain

⁵ Organisme National des Déchets Radioactifs et des Matières Fissiles Enrichies / Nationale Instelling voor Radioactief Afval en Verrijkte Splijtstoffen, Avenue des Arts 14, 1210 Brussels, Belgium

* Corresponding author. E-mail address: Thierry.mennecart@sckcen.be

Keywords:

Spent nuclear fuel, Leaching experiments, Fission products, Fast release, reducing conditions, H₂ effect, high pH conditions

1. Abstract

To study the dissolution of UOX spent nuclear fuel in a deep geological environment and the fast release of a selection of relevant radionuclides for long-term safety of this high level waste, leaching experiments were performed with spent nuclear fuel samples originating from the pressurized water reactors (PWRs) Tihange 1 and Gösgen with a similar burnup (50 – 55 MWd.kg_{HM}⁻¹) but different irradiation histories. Six experiments were conducted to investigate the effect of two critical parameters: (1) the highly alkaline environment caused by the presence of cementitious materials in the “Supercontainer design”, which is currently the reference design for the long-term management of the high-level nuclear waste forms in Belgium, and (2) the reducing conditions imposed by the presence of hydrogen from the corrosion of iron-based materials present in the engineered barriers. The experiments were performed using autoclaves under pressure from 1 to 40 bar with a pure Ar atmosphere or a mixture of H₂/Ar. Divided into two consecutive phases, the total experimental duration was about 1400 days. The Phase I provided mainly information about the fast release of the fission products while the perspective of the Phase II was to study the long-term evolution of the spent fuel matrix. During the leaching experiment, concentrations of a selection of radionuclides (²³⁸U, ¹²⁹I, ¹³⁷Cs, ⁹⁰Sr and ⁹⁹Tc) were monitored in solution and the amounts of Kr and Xe were measured in the gas phase. Based on results of the experiments conducted for up to 40 months (i.e. during Phase I of the experimental program), we observe that there is a continuous release of ¹³⁷Cs, ⁹⁰Sr and of the fission gases and a clear impact of the irradiation history on the release of certain fission products.

2. Introduction

Many countries with nuclear power plants consider the direct disposal of Spent Nuclear Fuel (SNF) in a deep geological repository as a safe long-term waste management option [1-3]. A safe solution has to be

defined in order to guarantee the effectiveness of the safety functions associated with the engineered barrier system during at least the thermal phase (a period of approximately ten thousand years) and to preserve the safety function of the natural barrier over hundreds of thousands up to a million years [4-7]. However, regardless of the design, groundwater intrusion through the geological and engineered barriers and consecutive contact with the SNF is considered, leading in the long-term to SNF alteration and the release of certain radionuclides into the environment to some extent. Consequently, it is very important to understand and to identify the dissolution mechanisms of the SNF under deep geological disposal conditions and to quantify the release of the radionuclides under such conditions.

The dissolution of the SNF and the release of the radionuclides (RNs) are a combination of two processes: a fast short-term release of segregated RNs occurring once the cladding has failed and water reaches the SNF, and a slow long-term release associated with the dissolution of the SNF matrix. Radionuclides that are segregated in voids like the gap between the cladding and the pellets or in the water-accessible grain boundaries, can be released fast upon contact with water.

The chemical composition of the solution in contact with the SNF and the redox conditions have a strong influence on the release behavior of the RNs [8-10]. The current reference design for the disposal of SNF in Belgium, the “Supercontainer design”, consists of a carbon steel overpack surrounded by a thick concrete buffer [11]. Based on a scoping calculation, a high pH solution was defined, representative of concrete pore water in the early stage of the concrete alteration [12]; this solution is called Young Cement Water with calcium (YCWCa, pH 13.5). Prior to the first contact with the SNF, the groundwater will also come in contact with the surrounding iron-based constituents, which will corrode generating H_2 and creating reducing conditions that can counteract the oxidative dissolution of the SNF.

In this context, a research program was launched to perform leaching experiments with representative UOX spent nuclear fuels from Pressurized Water Reactor (PWR) under deep geological repository conditions corresponding to the “Supercontainer design”. Two series of autoclave experiments were performed: one at SCK CEN (Belgium) with three fuel samples irradiated in the PWR Tihange 1 and one at KIT-INE (Germany) with three fuel samples irradiated in the PWR Gösigen. Because these fuels have a similar burnup, but a different Fission Gas Release determined in post-irradiation puncturing tests ($FGR_{puncturing}$) and Linear Power Rating (LPR), the leach tests allow to study also the effect of the irradiation history on radionuclide release. The experiments were carried out with the YCWCa under pure argon atmosphere or argon mixed with hydrogen to impose a defined hydrogen partial pressure, comparable to the pressure in the expected disposal conditions. One experiment was also performed with a bicarbonate medium, representative of a near neutral pH, to compare with literature data.

The experiments were performed in two phases. After the Phase I, lasting for about two years in five experiments and 40 months in a sixth experiment, the tests were continued in new autoclaves with freshly prepared YCWCa and bicarbonate leaching solution (Phase II) until a total experimental duration of about 1400 days. This paper focuses on the fast release of a selection of radionuclides and only reports the results of the Phase I.

3. Experimental

To impose the gas atmosphere and to determine the release of fission gases in the course of the experiment, the tests were performed in autoclaves. The autoclaves consist of a stainless steel pressure vessel and a titanium lid, firmly closed by two flanges, and an internal part (liner) made also of titanium with a total volume of 250 mL. The experiments were conducted at total pressures in the range 1 to 40 bar in a hot cell

at temperature (20 – 25°C). The top part of Figure 1 gives the experimental setup and the gas sampling cylinder at KIT-INE and the bottom part shows the experimental setup and the connections to the sampling containers at SCK CEN. The small differences in the setup have consequences for the sampling procedure (see section 3.4).

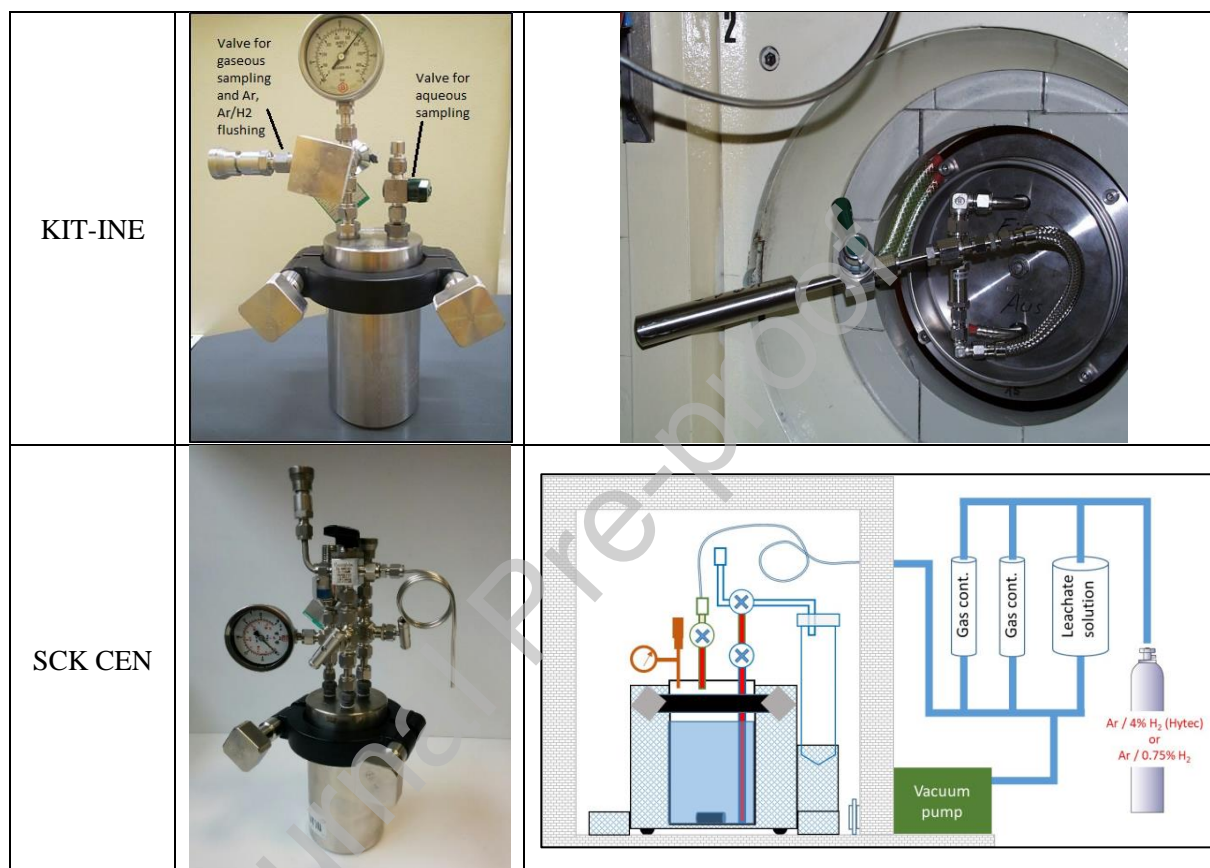


Figure 1: Experimental setup used at KIT-INE (top part) and at SCK CEN (bottom part).

3.1. Fuels

Two UOX spent nuclear fuels were studied. One fuel was irradiated in the Tihange 1 reactor (Belgium), denominated in this paper as ‘Th1’. The fuel was initially enriched with 4.25 % wt. of ^{235}U and was irradiated for 997 days in total. The burnup at the location of the tested fuel segments was $54.6 \text{ MWd.kg}_{\text{HM}}^{-1}$, the average LPR was 321 W.cm^{-1} [13]. The other fuel was irradiated in the Gösgen reactor (Switzerland), denominated as ‘Gos’. Initially enriched with 3.8 % wt. of ^{235}U , it was irradiated for 1226 days with an average LPR of 260 W.cm^{-1} and reached an average burnup of the fuel rod of $50.4 \text{ MWd.kg}_{\text{HM}}^{-1}$ [14, 15]. The Gos fuel sample was fabricated according to the NIKUSI process, and the Th1 fuel was produced according to the standard production route. Both fuels reached similar burnups; however, the higher average LPR of the Th1 fuel resulted in a higher centerline temperature during the irradiation. The relatively high

LPR and temperature during irradiation promoted the segregation of volatile fission products and resulted in the higher $FGR_{\text{puncturing}}$ of the Th1 fuel compared to that of the Gos fuel [16]. Table 1 summarizes the main characteristics of the spent nuclear fuels and their irradiation history.

Table 1: SNF characteristics.

Reactor name	Gösgen, Switzerland	Tihange 1, Belgium
Reactor type	PWR	PWR
Initial fuel enrichment (^{235}U)	3.80 %	4.25 %
Fabrication route	NIKUSI	Standard
Duration of irradiation (d)	1226	997
Number of cycles	4	2
Average burn-up ($\text{MWd.kg}_{\text{HM}}^{-1}$)	50.4	54.6
Average Linear Power Rate (W.cm^{-1})	260	321
Maximal Linear Power Rate (W.cm^{-1})	340	418
$FGR_{\text{puncturing}}$	$(8.3 \pm 0.9) \%$	$(14.1 \pm 0.9) \%$

Three segments of each fuel were prepared for the leaching experiments. Each sample was about 23 mm long, consisting of one whole and two half pellets within their cladding. The Gos fuel samples were cut using a low speed saw in absence of a cooling liquid in a hot cell under N_2 atmosphere; the Th1 fuel samples were prepared under air atmosphere using a tube cutter to cut the cladding and manually broken at the cutting plane.

The radionuclide inventories of the SNFs were obtained by calculation using the MCNP/CINDER codes [17, 18] for the Gos fuel and the Serpent 2 code for the Th1 fuel [19]. In addition, the inventories were determined by radiochemical measurement after total digestion of a neighboring sample of the Th1 fuel [20, 21] and of the Gos fuel [22]. The resulting inventory of Kr, Xe, ^{238}U , ^{129}I , ^{137}Cs , ^{90}Sr and ^{99}Tc is reported in Table 2 in $\text{g.g}_{\text{UO}_2}^{-1}$. The total amount of Kr and Xe at the end of the cooling time is also provided in Table 1, which amounted to 23 and 12 years for the Gösgen and the Tihange 1 fuels, respectively. After this period, a puncturing tests were performed to determine the gas phase composition in the plenum of the two fuel rod segments. The $FGR_{\text{puncturing}}$ was determined at $8.3 \pm 0.9 \%$ for the Gösgen fuel and $14.1 \pm 0.9 \%$ for the Tihange 1 fuel. The Xe to Kr molar ratio measured in the puncturing test was 12 ± 1 for the Gösgen fuel and 9 ± 1 in case of the Tihange 1 fuel. In comparison, the molar ratio Xe/Kr calculated for the total inventory was 10 ± 1 for both fuels, corresponding to a Xe/Kr mass ratio of 16 ± 1 for both fuels.

Table 2: Comparison of the calculated and measured inventories of the Gösgen and the Tihange 1 fuels for some isotopes of interest; the values are expressed in $g \cdot g_{UO_2}^{-1}$.

Isotopes	Gos		Th1	
	Calculated ⁽¹⁾	Measured ⁽²⁾	Calculated ⁽³⁾	Measured ⁽²⁾
Kr (total)	4.4×10^{-4}	$(4.0 \pm 0.3) \times 10^{-4}$	5.2×10^{-4}	Not available
Xe (total)	7.2×10^{-3}	$(6.2 \pm 0.1) \times 10^{-3}$	8.4×10^{-3}	Not available
⁹⁰ Sr	3.5×10^{-4}	$(5.6 \pm 0.5) \times 10^{-4}$	4.8×10^{-4}	$(5.1 \pm 0.3) \times 10^{-4}$
⁹⁹ Tc	9.7×10^{-4}	$(2.0 \pm 1.2) \times 10^{-4}$	1.1×10^{-3}	$(9.8 \pm 2.2) \times 10^{-4}$
¹³⁷ Cs	8.7×10^{-4}	$(1.0 \pm 0.1) \times 10^{-3}$	1.2×10^{-3}	$(1.2 \pm 0.1) \times 10^{-3}$
²³⁸ U	8.1×10^{-1}	$(8.5 \pm 0.6) \times 10^{-1}$	8.1×10^{-1}	$(8.1 \pm 0.1) \times 10^{-3}$
¹²⁹ I	2.1×10^{-4}	$(4.2 \pm 1.2) \times 10^{-4}$	2.2×10^{-4}	$(2.2 \pm 0.2) \times 10^{-4}$

⁽¹⁾ Calculated values using the MCNP/CINDER codes with respect to the reference date 13. March 2017. Uncertainties are not reported, but they are considered to be 2% for the uranium inventory and 7% for fission products, according to the assessment of [23].

⁽²⁾ Measured inventories on reference date 13. March 2017 [22] for Gos fuel and 26. September 2018 for Th1 fuel [21].

⁽³⁾ Values reported in [19] using Serpent 2 code with respect to the reference date 26. September 2018. Uncertainties are not reported, but they are considered to be 2% for the uranium inventory and 7% for fission products, according to the assessment of [23].

3.2. Leaching solution

Two leaching solutions were used: YCWCa and a bicarbonate solution. The bicarbonate solution was identical to the leachant used in the European program “FIRST-Nuclides” [24]. The composition of the YCWCa solution was defined by geochemical calculations assuming equilibrium between an Ordinary Portland Cement of type OPC/CEM I/LA/HSR and Boom Clay pore water [12]. The calcium concentration in the YCWCa was, however, reduced by 50 % in order to produce a leaching solution undersaturated in calcium, thus avoiding the precipitation of Ca-bearing compounds. The composition of the leaching solutions is given in Table 3. As part of a previous experimental program, we assessed the stability of the solution without SNF under other experimental conditions (FIRST-Nuclides: anoxic conditions with Th1 fuel [13]); the composition of the solution doesn't change after 1 year duration.

Table 3: Experimental composition of the leachate YCWCa and bicarbonate solutions.

mol.L ⁻¹	[Na]	[Ca]	[K]	[Al]	[Si]	[CO ₃ ²⁻]	[Cl]	pH
YCWCa	1.4×10^{-1}	3.8×10^{-4}	3.7×10^{-1}	6.0×10^{-4}	3.0×10^{-5}	3.0×10^{-4}		13.7 ± 0.2
Bicarbonate	2.0×10^{-2}					1.1×10^{-3}	1.9×10^{-2}	8.5 ± 0.2

3.3. Atmosphere

Different gas atmosphere compositions were chosen to assess the effect of various concentrations of dissolved hydrogen on the spent nuclear fuel dissolution. In the near-field of the SNF disposal system, the long-term hydrogen concentration will be imposed by multiple sources of H₂ production (corrosion of

cladding, assembly metal, iron insert, etc...). The experiments were performed considering a dissolved H₂ concentration in the range $2.4 \times 10^{-4} \text{ mol.L}^{-1}$ to $2.5 \times 10^{-3} \text{ mol.L}^{-1}$. This range of concentration was based on the current expected corrosion rate [25] and considered as a relatively low estimation of the expected *in situ* hydrogen concentration. In order to test the hydrogen effect and the consequence of a potential higher corrosion rates on the SNF leaching, experiments were performed with a dissolved H₂ concentration up to $2.5 \times 10^{-3} \text{ mol.L}^{-1}$. The concentration of $2.4 \times 10^{-4} \text{ mol(H}_2\text{).L}^{-1}$ was obtained using a gas mixture of 8 %H₂/Ar under 3.75 bar in the experiment with the Gos fuel and using a gas mixture of 0.75 %H₂/Ar under 40 bar in the experiments with the Th1 fuel. To reach the higher dissolved hydrogen concentrations, experiments were performed with 8 %H₂/Ar at 40 bar pressure with a Gos fuel sample ($2.5 \times 10^{-3} \text{ mol(H}_2\text{).L}^{-1}$) and with 4 %H₂/Ar at 40 bar in an experiment with a Th1 fuel sample ($1.3 \times 10^{-3} \text{ mol(H}_2\text{).L}^{-1}$). In addition to these four experiments, a Gos fuel sample was leached under pure Ar atmosphere to compare reducing and anoxic conditions. Furthermore, a Th1 fuel sample was leached under the low H₂ hydrogen concentration in contact with the bicarbonate solution to determine the impact of the presence of carbonate known to promote the dissolution of uranium by complexation of U(VI) and to compare the results with literature data. Table 4 gives the terminology and the experimental details of the experiments. The redox potential was not measured in any of the experiments, but the presence of hydrogen overpressure in five of the six experiments indicates strongly reducing conditions in these tests.

Table 4: Experimental matrices.

Exp.	Leaching solution	Atmosphere	Total pressure (bar)	H ₂ partial pressure (bar)	mol(H ₂).L ⁻¹
40 / 3.2H – Gos	YCWCa (pH 13.5)	8 % H ₂ /Ar	40	3.2	2.5×10^{-3}
3.75 / 0.3H – Gos	YCWCa (pH 13.5)	8 % H ₂ /Ar	3.75	0.3	2.4×10^{-4}
1 – 40 / 0 – Gos	YCWCa (pH 13.5)	Ar	1 – 8*	0	0
40 / 1.6H – Th1	YCWCa (pH 13.5)	4 % H ₂ /Ar	40	1.6	1.3×10^{-3}
40 / 0.3H – Th1	YCWCa (pH 13.5)	0.75 % H ₂ /Ar	40	0.3	2.4×10^{-4}
40 / 0.3H – Th1 – Bic	Bicarbonate solution (pH 8.5)	0.75 % H ₂ /Ar	40	0.3	2.4×10^{-4}

SNF from Tihange 1 is denoted as Th1 and Gösgen is denoted as Gos

* 1 bar until 497 days, 8 bar between 497 and 785 days

3.4. Leaching test procedure

The SNF samples were mounted on titanium sample holders to ensure the contact of both cutting planes with the solution and then placed in the autoclaves. After closing the autoclaves, they were purged with Ar or the corresponding Ar/H₂ gas mixtures. Then, the autoclaves were filled with the leachate (Gos: $219 \pm 1 \text{ mL}$, Th1: $200 \pm 1 \text{ mL}$) through a valve in the lid, and the autoclaves were pressurized. This corresponds to the start of the leaching experiment (t_0).

During the experiments, regular samplings of the gas and liquid phases (10 mL) were performed to measure the concentration of the radionuclides released in solution and the fission gases in the headspace of the autoclaves. In addition, after 1 day (t_0+1d) in the experiments with the Gos fuel and after 5 days (t_0+5d) in the case of the Th1 fuel, the leaching solutions and the gas phases were completely renewed in order to reduce the activity of the leachate (mainly due to cesium) and to decrease the concentration of radionuclides

that could be initially released from a pre-oxidized layer on the surface of the samples that may mask any smaller further release.

For the experiments with Th1 fuel this so-called washing step and all next solution and gas samplings were performed with the autoclave closed. The lid was equipped with a valve for the gas sampling of the headspace and a second valve with a titanium tube, long enough to reach up to the bottom of the vessel, which allowed to take liquid phase samples. This system allowed to empty the vessel almost completely during the washing step (1 mL remains in the autoclave) and to take samples later in the experiment without intrusion of air. The samplings were performed under pressure but a decrease of the pressure during to the sampling to 35 – 36 bar cannot be avoided. After the sampling, the pressure was adjusted to the target value.

In the experiments with the Gos fuel, once the gas sampling was performed, the pressure was totally released before the solution samples were taken. In these tests, the solution samplings and the extraction of the leachate were performed using a syringe passing through a valve [26, 27]. With this method, the gas phase was completely renewed after each sampling. Air intrusion was avoided by a permanent Ar flushing of the autoclave. The total pressure of the autoclaves was afterwards adjusted to the target value.

Whatever the protocol for sampling, procedures have been established to avoid any dead volume (solution in the Ti tube or gas phase) once the pressure was reset to the target value.

For the experiments with the Th1 samples, the pressure was reduced to 4 bar between the sampling at t_0+586d until the end of the Phase I (t_0+733d). Initially imposed to overcome a period of reduced lab activity due to the COVID-19 pandemic operation restrictions, this pressure reduction provided the opportunity to evaluate the influence of the pressure decrease by a factor 10 on the leaching behavior. For the experiments with the Gos fuel, Phase I lasted 763 days (40 / 3.2H – Gos), 1205 days (3.75 / 0.3H – Gos) and 785 days (1 – 40 / 0 – Gos).

At the end of the experiments, the Ti-liners were rinsed with $1 \text{ mol.L}^{-1} \text{ HNO}_3$ to measure the amount of radionuclides sorbed on the walls. The acid solution was in contact with the Ti-liners for 1 day and 1 week in the experiments with the Gos and Th1 fuels, respectively. Figure 2 provides information about the experimental timeline for the two series, the total pressure and the composition of the atmosphere.

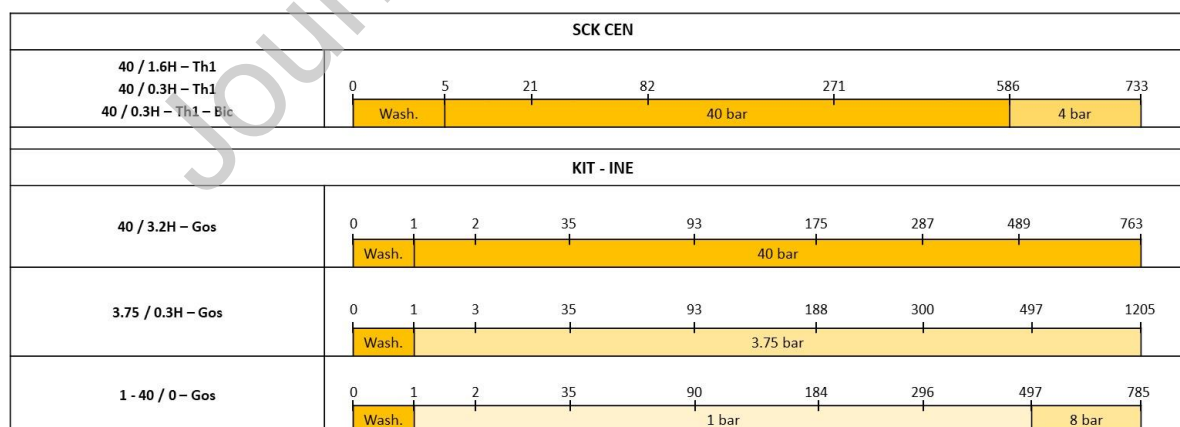


Figure 2: Timeline with the sampling intervals in days relative to the start of the experiment and the total pressure imposed during Phase I of the leaching experiments. 'Wash.' refers to the washing of the segments, explained in section 3.4.

3.5. Solution and gas analyses

The gas samples were analyzed using a multipurpose mass spectrometer (GAM 400, InProcess Instruments), equipped with a quadrupole mass analyzer, Faraday and secondary electron multiplier detectors for the Gos fuel (KIT-INE) and a Hiden Analytical HPR-70 quadrupole mass spectrometer for the Th1 fuel (SCK CEN). H₂, N₂, O₂, Ar, (and CO₂ at KIT-INE), as well as the Kr and Xe isotopes were measured. These samplings also allowed checking the possible variation of the composition of the initial Ar/H₂ mixture and to monitor any air intrusion by checking the N₂ content. No significant contribution of N₂ was observed during the whole experimental duration for all experiments demonstrating the tightness of the autoclaves.

A selection of radionuclides which are relevant for the long-term safety of SNF, or which are studied to understand the SNF dissolution were measured in aqueous solution. This paper reports the results for ²³⁸U, ¹²⁹I, ¹³⁷Cs, ⁹⁰Sr and ⁹⁹Tc.

For the solution samples, one aliquot was used for the determination of the uranium isotopes and ⁹⁹Tc by inductively coupled plasma-mass spectrometry (ICP-MS), a high-resolution device was used at KIT-INE. Iodine was measured also by ICP-MS, but only at SCK CEN. The gamma emitters such as ¹³⁷Cs were measured by gamma spectroscopy and ⁹⁰Sr was measured by liquid scintillation counting (LSC). A complete description of the methodologies can be found in [20, 21]. Since no difference was observed between non-filtered and ultra-filtered solutions in the experiment with the Gos fuel, only the non-filtered results are presented in this paper. The pH was measured in the Gos experiments using the solution aliquot and no noticeable pH evolution was observed at the end of the experiments (pH 13.6 ± 0.2).

The concentrations and other results in this paper are presented with error bars corresponding to the 95 % confidence intervals.

4. Results

4.1. Fission gas release

The evolution of the total accumulated amount of Kr and Xe released in the gas phase as a function of the leaching time is presented in Figure 3. For all experiments, Kr and Xe showed a fast initial release in the first 200 days and a continuous slow release in the remaining duration of the leaching experiment.

The values obtained in the experiments with the Th1 samples were close to each other. The highest release was observed for the experiment with the highest H₂ partial pressure in presence of YCWCa (40 / 1.6H – Th1), and the lowest release was obtained with the low H₂ partial pressure in presence of the bicarbonate solution (40 / 0.3H – Th1 – Bic). The third experiment, with the low H₂ content in YCWCa (40 / 0.3H – Th1) showed an intermediate release. After 733 days, the difference of the cumulative release between the three experiments was small. Hence, very little influence of hydrogen or the solution composition was observed on the Kr and Xe release at the end of the leaching experiments with the Th1 fuel.

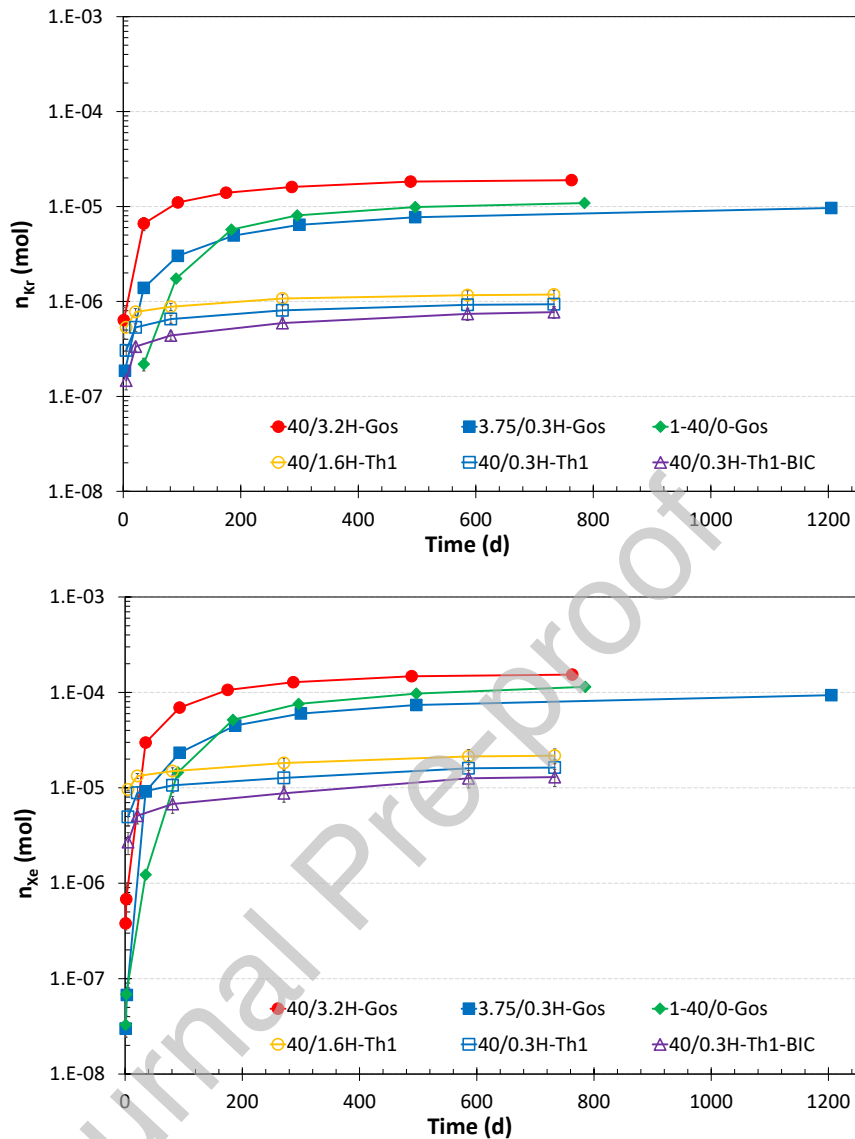


Figure 3: Evolution of the moles of Kr (top) and Xe (bottom) released as a function of the time (data below the detection limit were omitted).

For the Gos fuel samples, the Kr and Xe release was significantly higher for the experiment with the highest total pressure (40 / 3.2H – Gos) compared to the two other experiments. The three experiments were performed in the same medium (YCWCa), so the difference can be attributed only to the total pressure (1, 3.75 or 40 bar) of the imposed atmosphere, and possibly to the H_2 partial pressure. After this period, the release of Kr and Xe was quite similar in the experiments 3.75 / 0.3H – Gos and 1 – 40 / 0 – Gos, and the Kr and Xe release was about 10 times larger for the Gos fuel than for the Th1 fuel.

4.2. Uranium-238

The evolution of the aqueous ^{238}U concentrations is plotted in Figure 4-a and the repartition of uranium release from the SNF between the amount measured in solution and sorbed on the Ti-liners in Figure 4-b. For most experiments, the concentrations fluctuated strongly in the range $10^{-8} - 10^{-6} \text{ mol.L}^{-1}$. Such a scatter in aqueous uranium concentrations has often been observed in experimental studies on dissolution of spent nuclear fuels under reducing conditions [28]. During all samplings of the three experiments with Gos fuel samples, it was tested whether measured uranium concentrations in solution would be affected by colloid formation. Since measured uranium concentrations of unfiltered and filtered (after 10 kDalton ultrafiltration) were the same within the analytical uncertainty, an effect of colloids present in solution as the dominant reason for the scatter was not considered.

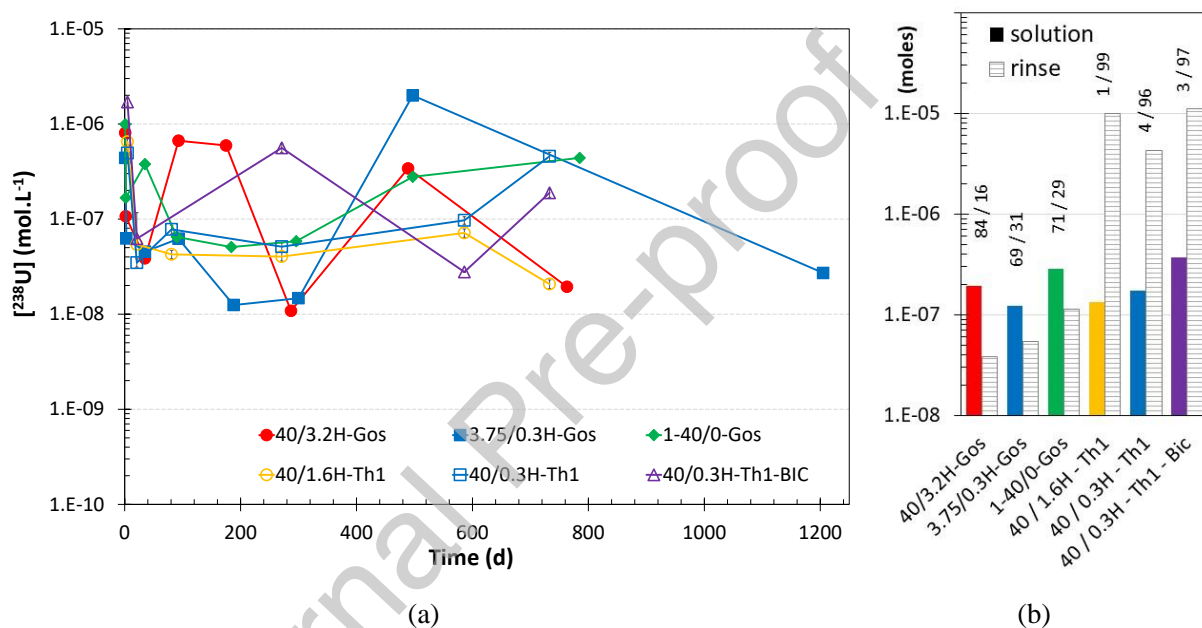


Figure 4: (a) Evolution of the concentration of ^{238}U as a function of the leaching time and (b) ^{238}U moles in the leaching solution compared with the amount measured in the rinse solution (sorbed on the wall). Values above the bars are the mole ratio solution/rinse.

4.3. Iodine-129

The ^{129}I results correspond only to the experiments with the Th1 fuel samples. The concentrations in the experiment with the bicarbonate solution were higher than in the experiments with the YCWCa (Figure 5). The H_2 partial pressure did not affect the release of iodine, as the concentrations in YCWCa with 1.6 and 0.3 bar H_2 were not much different. In the three experiments, there was a high initial release ($t_0+5\text{d}$), with a concentration of about $10^{-5} \text{ mol.L}^{-1}$. After the renewal of solution, lower and rather stable concentrations are observed in the bicarbonate solution until the end of the experiments; around $10^{-5} \text{ mol.L}^{-1}$. In the two experiments with the YCWCa, even lower concentrations are measured after 21 days, and we observe a slight increase until 271 days and then a decrease in concentrations. The cause for the iodine concentration drop is not clear since iodine cannot volatilize from the autoclave nor being removed from solution by precipitation of an iodine bearing compound.

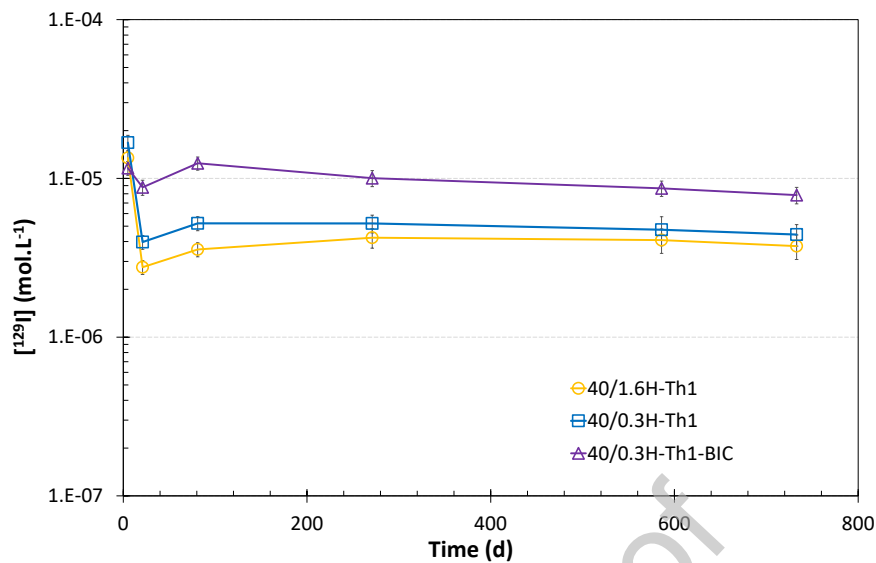


Figure 5: Evolution of the concentration of ^{129}I as a function of the leaching time in the experiments with the Th1 fuel samples.

4.4. Cesium-137

For the Th1 fuel, several cesium isotopes (^{133}Cs , ^{134}Cs , ^{137}Cs) were analyzed in solution and most of the cesium released in solution was due to ^{133}Cs (stable) and ^{137}Cs (half-life 30 years). The concentration of ^{134}Cs was several orders of magnitude lower, in-line with the expected low residual content of ^{134}Cs after almost 25 years of cooling time. In the Gos samples, only ^{137}Cs was measured, therefore the discussion focuses on this isotope. The concentration of ^{137}Cs as a function of time is plotted in Figure 6. In all experiments, the concentration increased as a function of time, except for the experiments with Th1 fuel samples in contact with YCWCa (40 / 1.6H – Th1 and 40 / 0.3H – Th1), where we observe a high initial release at $t_0+5\text{d}$ followed by a drop of concentration after 21 days due to the renewal of solution. Afterwards, the concentrations continues to increases slightly with the exception of the last sampling in experiment 40 / 1.6H – Th1. It looks like the fast Cs release from the Th1 fuel sample is achieved during the first five days under hydrogen and in contact with the high pH solution while more time is needed under the other conditions or another fuel, as it is the case in the experiment under anoxic conditions, 1 – 40 / 0 – Gos, where the concentration approaches a steady state ‘only’ after 200 days. Cesium was measured in the rinse solution of the Ti-liners at the end of the experiments. The sorbed fractions represented less than 2 % and 0.5 % of the total amount of Cs release in the experiments with the Th1 and Gos fuels, respectively.

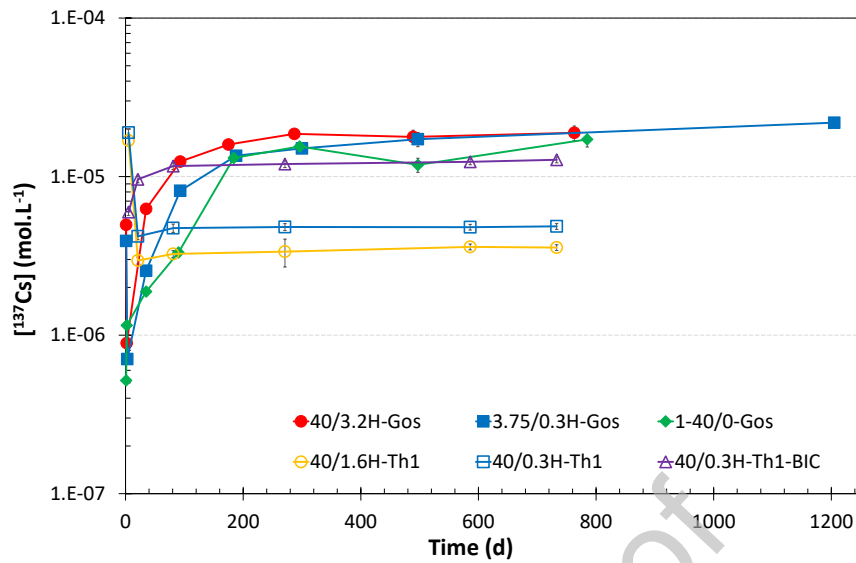


Figure 6: Evolution of the ^{137}Cs concentration as a function of the time.

4.5. Strontium-90

Like for cesium, the ^{90}Sr release is influenced by the experimental conditions and the fuel (Figure 7-a). Although a continuous increase of the concentration is observed for all experiments, the concentrations are one to two orders of magnitude higher in the experiments with the Th1 fuel than with the Gos fuel, and for the same fuel (Th1), one order of magnitude higher in bicarbonate solution than in the YCWCa. Moreover, a significant fraction of the Sr was sorbed on the Ti-liners in the experiments with the Th1 fuel, whereas this sorbed fraction was lower for the Gos fuel (Figure 7-b). The lower Sr concentrations in solution for the Gos fuel is thus not a consequence of the sorption, but the higher Sr concentration for the Th1 fuel may have induced more sorption.

Over the entire experimental duration neither the imposed atmosphere nor the total pressure seems to have a considerable influence on the release of strontium since the three experiments with the Gos fuel samples provided similar results in presence or absence of hydrogen, as the two experiments with Th1 fuel in YCWCa with different hydrogen concentrations also resulted in a similar Sr release.

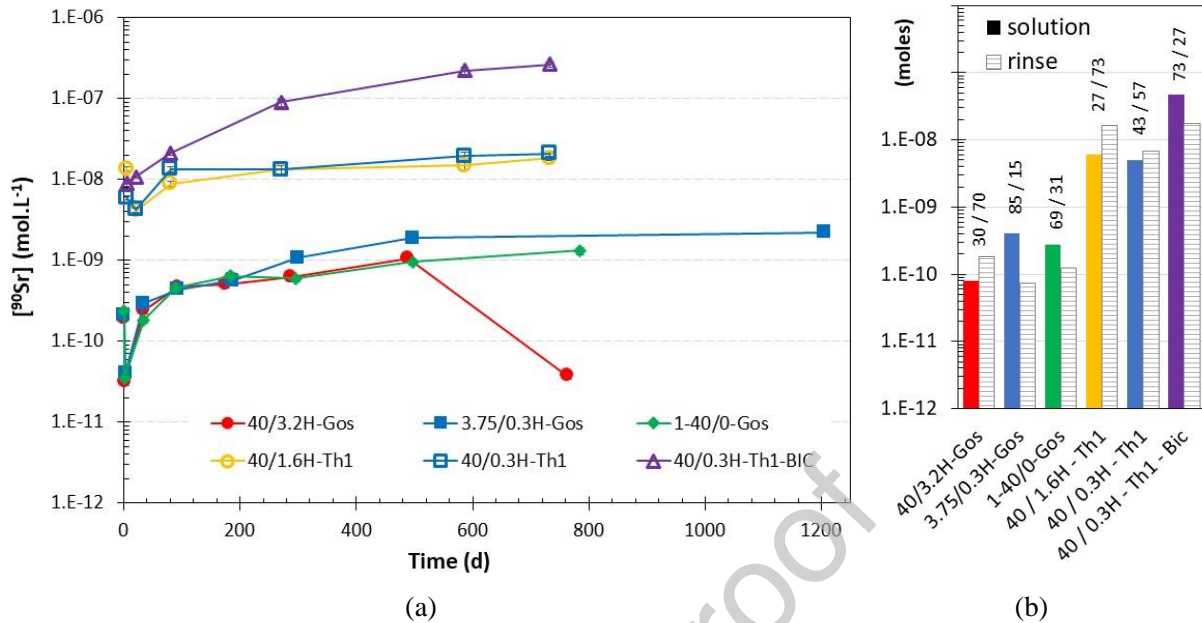


Figure 7: (a) Evolution of the ^{90}Sr concentration as a function of the time and (b) ^{90}Sr moles in the leaching solution compared with amount measured in the rinse solution (sorbed on the wall). Values on the top of the bars are the moles ratio solution/rinse.

4.6. Technetium-99

After a fast initial release in solution, the technetium concentrations drop to $10^{-8} \text{ mol.L}^{-1}$ in the three experiments with the Th1 fuel and to even lower values with the Gos fuel, as a consequence of the solution renewal (Figure 8-a). Afterwards, the concentrations in the experiments with the Gos fuel samples are close to or below the detection limit, leading to a scattered evolution. In the experiments with the Th1 fuel, the technetium concentrations remain stable at about $10^{-8} \text{ mol.L}^{-1}$ in both experiments at high pH while we observe a continuous increase to $3 \times 10^{-7} \text{ mol.L}^{-1}$ in bicarbonate solution at $t_0+733\text{d}$. Furthermore, a minor increase is also observed in the YCWCa at $t_0+733\text{d}$, which could be attributed to the lower pressure imposed at that time (4 bar instead of 40 bar between $t_0+586\text{d}$ and $t_0+733\text{d}$), inducing a lower H_2 concentration dissolved in solution and decreasing the protective effect against the oxidation of technetium. A negligible amount of technetium is found on the Ti-liners in the experiments with the Gos fuel, between 1 % and 5 % of the total amount of Tc released, while the sorbed fraction represented 10 – 41 % in the experiments with the Th1 fuels (Figure 8-b).

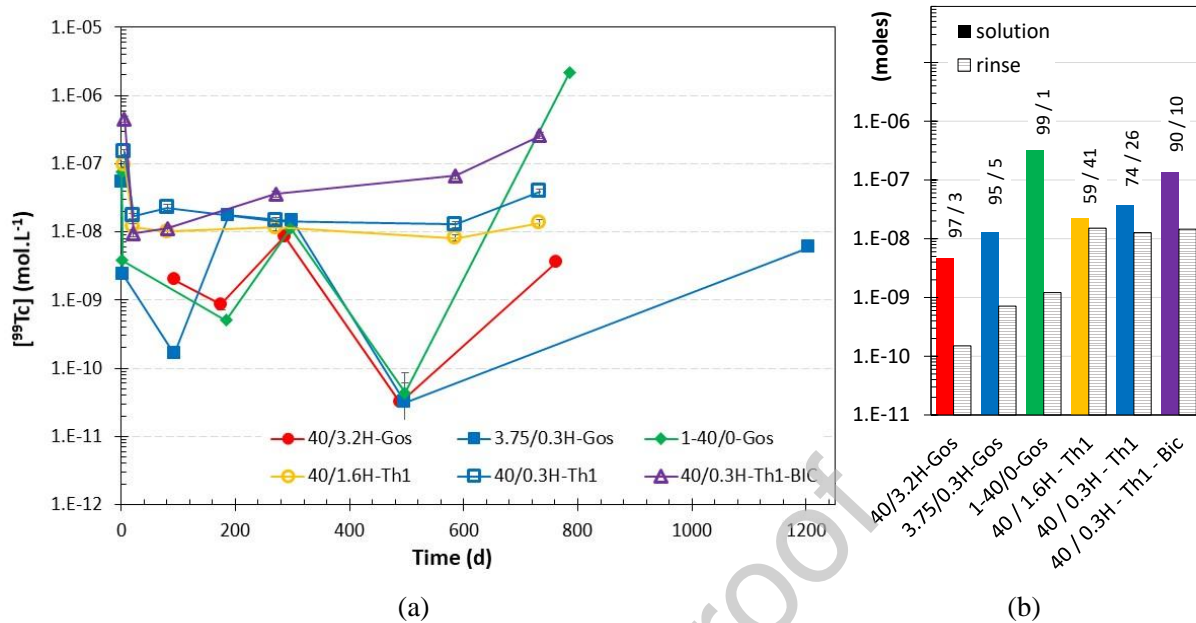


Figure 8: (a) Evolution of the ^{99}Tc concentration as a function of the time and (b) ^{99}Tc moles in the leaching solution compared with amount measured in the rinse solution (sorbed on the wall). Values above the bars are the moles ratio solution/rinse. No data are available before $t_0+93\text{d}$ in the experiment 40 / 3.2H – Gos (data below the detection limit are omitted).

5. Discussion

The concentrations of dissolved radionuclides are used to calculate their Fraction of radionuclide Inventory in the Aqueous Phase (FIAP). Each FIAP value corresponds to the ratio between the number of moles of a specific radionuclide released in solution at a certain time over its total amount in the initial SNF sample. The FIAP thus quantifies the extent of dissolution regardless of the surface area of the sample, which is a difficult parameter to accurately/correctly evaluate [29]. Considering the washing steps with the complete renewal of solutions, the samplings as a function of time (removal of small fraction of the released inventory each time) and the possible sorption of some radionuclides on the Ti-liner, the amount of moles measured in solution at a specific sampling step does not correspond to the total moles released from the SNF from the start of the experiment. Consequently, to completely cover the inventory released from the SNF, the cumulative FIAP (CumFIAP) is introduced, which takes into account all measured fractions from the start of the experiment until a specific duration.

Uranium release

As mentioned in section Results, aqueous uranium concentrations display a considerable scatter. In experimental studies on dissolution of spent nuclear fuels under reducing conditions such a dispersion is commonly observed and often attributed to the dissolution of pre-oxidized surfaces of the spent nuclear fuel samples [28]. It can be assumed that in the short period between the preparation of the Gos and Th1 fuel samples (cutting) and the start of the dissolution experiments, the SNF samples were in contact with air and the exposed surface area could thus be oxidized to some extent. Alternatively, we interpret this scatter of

measured uranium concentrations as a consequence of the speciation of U(IV) in the experiments. A considerable dispersion of aqueous concentrations for more than 100 days in thermodynamic solubility studies dealing with U(IV) and other tetravalent actinide (An(IV)) solid phases is well known (e.g. [30, 31]). In these thermodynamic studies, the scatter is attributed to artefacts related to the predominance of the neutral species $U(OH)_4(aq)$ and $An(OH)_4(aq)$. A conceivable explanation for the fluctuation in uranium concentration could be the presence of small colloidal species adherent to the vessel walls, which are not removed from the initial solution by filtration.

The fraction of uranium sorbed on the Ti-liner was much larger for the Th1 samples (90 %) than for the Gos samples (30 %). As it is not known when the sorption occurred, the sorbed fraction was added arbitrarily to the sampling that coincided with the rinsing. This causes a very high increase of the CumFIAP(^{238}U) at t_0+733d for the experiments with the Th1 fuel samples (Figure 9).

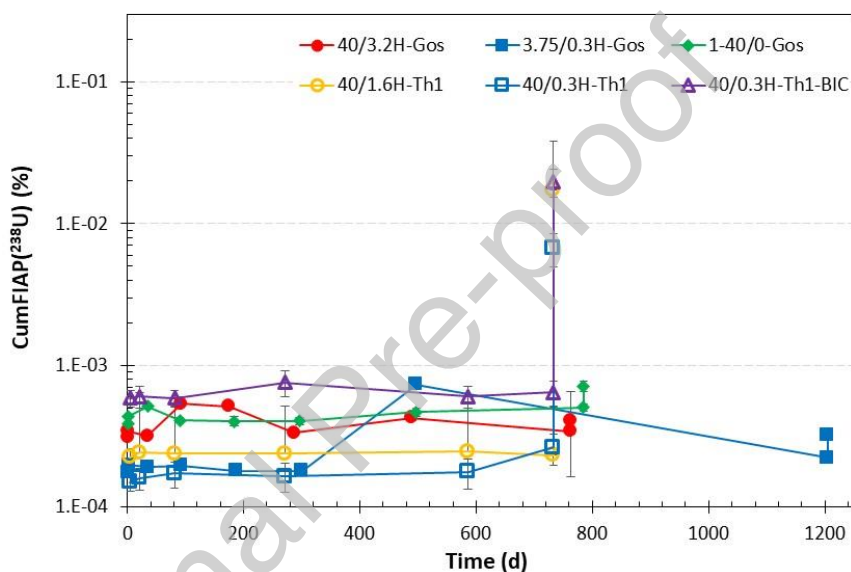


Figure 9: Evolution of the CumFIAP(^{238}U) (in %) as a function of the leaching time including the rinsing of the liners at the end of the experiments.

Expressing the data as CumFIAP levels out the fluctuations of the concentrations and reveals some meaningful trends. For the Th1 fuel, the cumulated uranium release appears to be higher in the bicarbonate medium than in the YCWCa, but considering the sorbed fraction, the difference becomes much smaller. For the Gos fuel, the cumulated uranium release is slightly higher for the test without hydrogen gas, 1 – 40 / 0 – Gos, suggesting the stabilizing effect of hydrogen on the fuel matrix.

Kr and Xe release

The evolution of Kr and Xe released into the gas phase does not show any significant effect of the H_2 partial pressure on the fission gas release during leaching ($FGR_{leaching}$). $FGR_{leaching}$ results of the experiments with the Th1 fuel are almost the same within error despite their differences in the H_2 partial pressure between 0.3 and 1.6 bar. Similar $FGR_{leaching}$ values are observed in the experiments with Gos fuel under 0.3 bar H_2 gas pressure (3.75 bar total pressure) and pure Ar atmosphere (1 bar total pressure). The relatively high $FGR_{leaching}$ values in experiment 40 / 3.2H – Gos compared to the two other experiments with Gos fuel are

interpreted as a consequence of the high total pressure in this experiment (40 bars) rather than a consequence of the H_2 partial pressure (3.2 bars). A more striking feature is the clear difference of the total moles of fission gases released during leaching of the two fuels (Figure 3). During the leaching, a higher amount of gases is released by the Gos fuel than by the Th1 fuel. This difference can be attributed to the different irradiation histories and especially to the difference in LPR values, because the LPR has an impact on the physical and chemical properties of the SNF. Indeed the LPR and the $FGR_{\text{puncturing}}$ values are considerably higher for the Th1 than those of the Gos fuel, despite comparable burnup values. When summing-up each fraction released during irradiation into the rod plenum (determined in the puncturing test) and each fraction released in the course of the leaching experiment, the total amount of Kr and Xe released are in the same range for both fuels (Figure 10). Because the total amount of Kr and Xe in the initial fuel inventory is similar for the two fuels, it may be assumed that the Th1 fuel releases less fission gases throughout the leaching experiment, because it has released a large fraction of the fission gases in the rod plenum already during in-reactor service, but further detailed assessment of the local distribution of Xe in both fuels would be needed to corroborate this assumption.

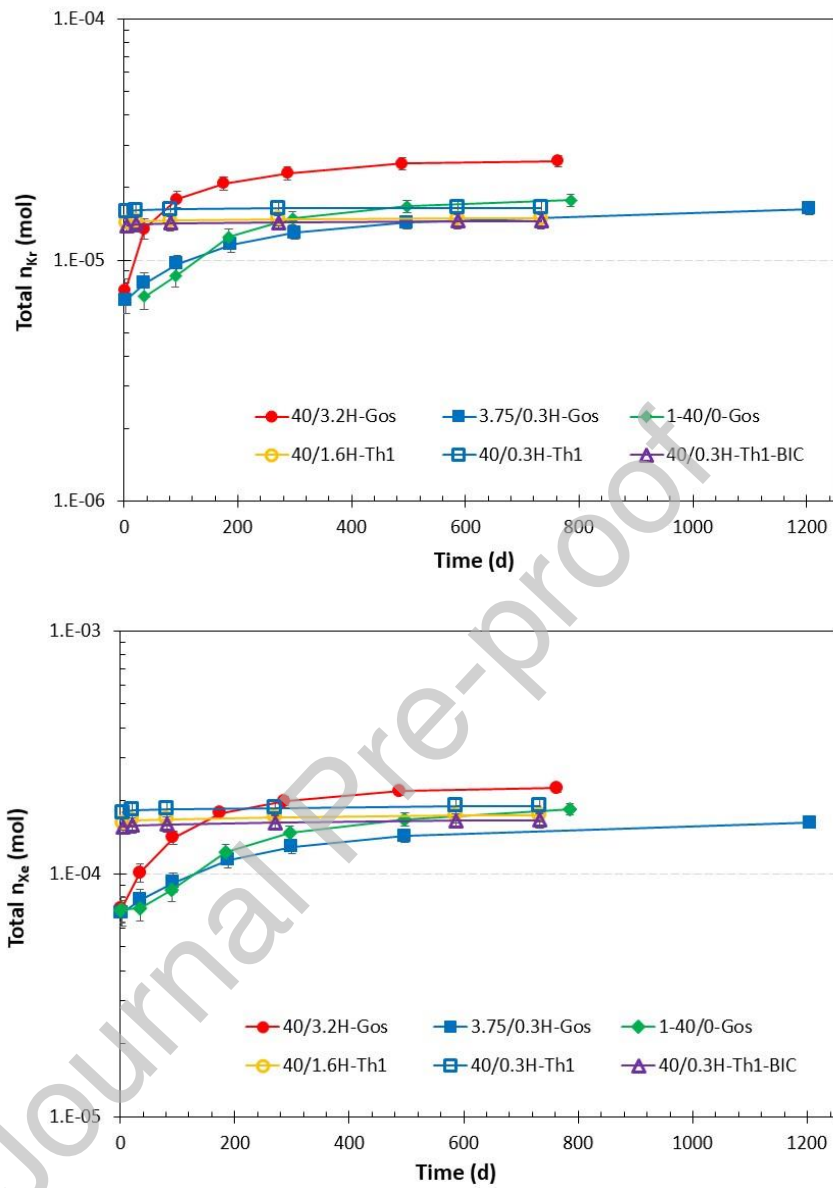


Figure 10: Evolution of the total amount of Kr (top) and Xe (bottom) as a function of the time, including the fission gas release upon the puncturing test.

Comparable with the FIAP of the dissolved radionuclides, the Fraction of fission gas Inventory released in the Gas phase (FIG) is the ratio between the total amount of a specific element released in the autoclave over its total inventory in the fuel sample. The FIG values for Kr and Xe are reported in Table 5, which also gives the FIG including $FGR_{\text{puncturing}}$ measured in the puncturing tests (FIG_{total}). Although the linear power was larger for the Th1 fuel, the FIG values are higher for Gos fuel than for Th1 fuel. Even when the $FGR_{\text{puncturing}}$ values are added to the FIG, FIG_{total} values of the experiments with Gos fuel are higher compared to those of the Th1 fuel. It seems that fuel properties such as reactor operation parameters (e.g. LPR) and fuel fabrication method affect the $FGR_{\text{puncturing}}$, but not the total amount of released Kr and Xe.

Intensive post-irradiation fuel examinations are required to clearly identify the keys parameters involved in the fission gases repartition in the fuel matrix. The FIG values for Kr and Xe obtained with the Gos fuel were very similar to those already published using the same fuel rod in contact with a bicarbonate solution under hydrogen atmosphere [14]. Even a higher value ($FIG(Xe) = 28 \pm 1 \%$) was obtained in an experiment conducted with fragments (1 – 2 mm) of high burnup fuel (78 MWd.kgU^{-1}) leached during 400 days in a bicarbonate solution under H_2 [32].

Table 5: Fission gas inventory release, FIG (in %), for Kr and Xe at the end of the experiments and the penultimate sampling for the Gos fuel (corresponding test durations are reported) for the two fuels under the six experimental conditions. The values in brackets (FIG_{total}) include the fission gas release measured in the puncture test (8.3 % Gos fuel and 14.1 % for Th1 fuel).

FIG (%)	Gos			Th1		
	40 / 3.2H	3.75 / 0.3H	1 - 40 / 0	40 / 0.3H Bic	40 / 0.3H	40 / 1.6H
Duration (d)	489	497	497	733	733	733
	763	1205	785			
Kr	23.9 ± 1.5 (30.9 ± 1.7)	10.4 ± 0.2 (17.4 ± 0.7)	13.0 ± 0.7 (20.0 ± 1.0)	1.3 ± 0.1 (15.9 ± 1.0)	0.9 ± 0.1 (15.5 ± 1.0)	0.9 ± 0.1 (15.5 ± 1.0)
	24.8 ± 1.5 (31.8 ± 1.7)	13.1 ± 0.2 (20.1 ± 0.7)	14.3 ± 0.8 (21.3 ± 1.0)			
Xe	18.9 ± 0.3 (27.5 ± 0.4)	9.8 ± 0.2 (18.3 ± 0.3)	12.5 ± 0.7 (21.0 ± 0.7)	2.3 ± 0.1 (16.3 ± 1.0)	1.5 ± 0.1 (15.5 ± 1.0)	1.4 ± 0.1 (15.4 ± 1.0)
	19.6 ± 0.3 (28.1 ± 0.4)	12.4 ± 0.2 (20.9 ± 0.3)	14.7 ± 0.7 (23.2 ± 0.8)			

In addition, the ratio Xe/Kr is apparently influenced by fuel properties such as the LPR. The ratio Xe/Kr of the gases released during leaching indicates a distinct behavior depending on the type of fuel (Figure 11).

In case of the Th1 fuel samples, the ratios are in the range 15 – 19, which is higher than the molar ratio of 10 ± 1 in the total inventory. The Xe/Kr molar ratio determined during the puncturing test (9 ± 1) is slightly lower than the ratio calculated for the total inventory, but the difference is not significant given the uncertainties of the values. Such a relatively high Xe/Kr ratio measured during the leaching is interpreted as a preferential release from zones with elevated Pu content, such as the peripheral rim zone.

In contrast to the fission gas release pattern of the Th1 samples, the Xe/Kr ratio for the Gos fuel shows a considerable variation with time in the first 200 days towards the ratio of the inventory after one year. From the initial values (< 1), the ratios increase until reaching values of about 10 for the experiment 3.75 / 0.3H – Gos and 1 – 40 / 0 – Gos while the ratio reaches a maximum of 8.1 (last sampling) in the experiment 40 / 3.2H – Gos. Such an increase of the Xe/Kr ratio during leaching is also observed in leaching experiments with a neighboring fuel sample from the same Gos fuel rod [14]. This would suggest that Kr was preferentially leached in the first 200 days. The incongruent release of the fission gases at the early stage of the experiment was attributed by the authors to different trapping sites of Xe and Kr in the spent nuclear fuel, where the Kr would be located in more water accessible sites such as grain boundaries.

Combined with the molar ratio of about 12 ± 1 , determined during the puncturing test and the ratio calculated in the total inventory of 10 ± 1 , there is also a balance in the gas released, but the behavior is quite distinct from that of the experiments with Th1 fuel.

For the Gos fuel, the Xe/Kr molar ratio tends to reach the ratio determined upon the puncturing test, while for the Th1 fuel, this ratio is apparently constant at a value significantly higher than the Xe/Kr ratio of the fuel inventory and the ratio determined in the puncturing test. The difference between the two fuels might be attributed to their different irradiation histories.

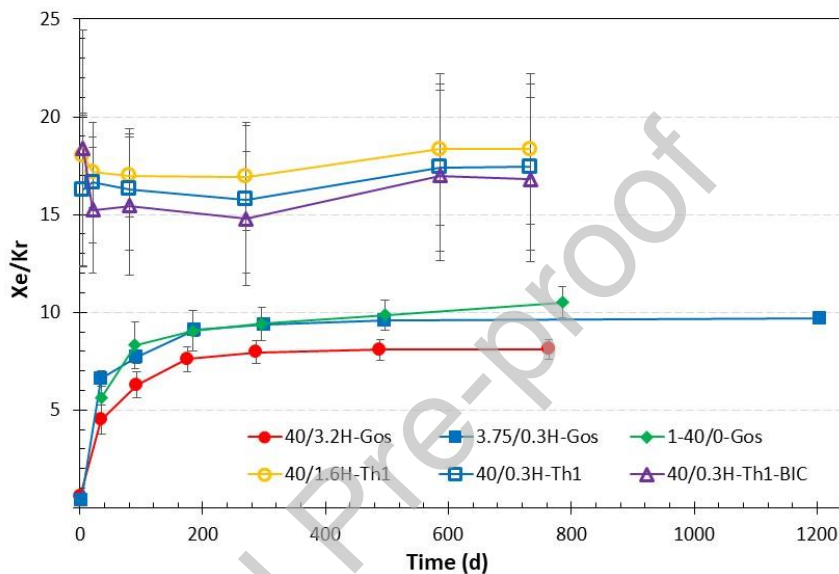


Figure 11: Evolution of the molar ratio Xe/Kr as a function of the leaching time (data below the detection limit were omitted).

Iodine release

As described in section 4.3, the iodine concentrations are higher in the bicarbonate solution than in the YCWCa (Figure 5). This would suggest that the iodine release is more sensitive to the composition of the leaching medium (such as pH and carbonate concentration) than to the redox conditions imposed by the hydrogen gas. Nevertheless, at the end of the experiment, the cumulative release of iodine CumFIAP(^{129}I), derived from the concentrations using the same methodology as for uranium, is very similar in the three experiments (Figure 12). Therefore, it is likely that the difference observed in the concentrations could be the consequence of a faster iodine release during the washing step rather than a medium composition effect.

The release of volatile elements, in particular the release of iodine, is often correlated to the fission gas release, usually determined in puncturing tests [33]. The evolution of the total release of the fission gases including the fraction from the puncturing test is plotted together with the CumFIAP(^{129}I) in Figure 12.

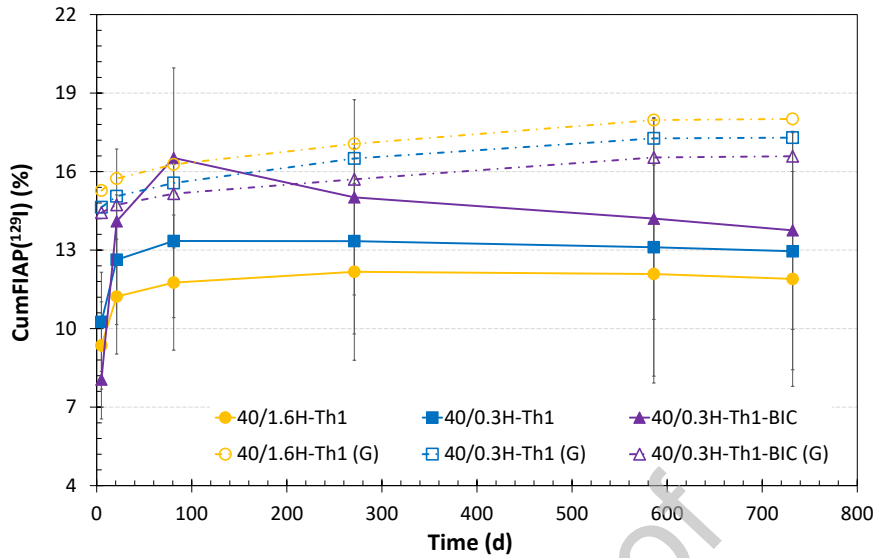


Figure 12: Evolution of the CumFIAP(^{129}I) as a function of the leaching time in the experiments with the Th1 fuel. The dotted lines correspond to the evolution of the sum of the fission gas released (Kr + Xe) during the experiment and the fission gas release upon puncturing test (14.1 % $FGR_{\text{puncturing}}$).

The highest release was observed in the bicarbonate solution where the FGR_{total} value was reached after the second sampling ($t_0+21\text{d}$). In the experiments with the YCWCa, the CumFIAP(^{129}I) values never reach this threshold and stay below 14 %. The lowest release is observed for the experiment with the highest H_2 partial pressure (40 / 1.6H – Th1). As a consequence of the decrease of the concentration as a function of the time, the CumFIAP(^{129}I) decreases as well. After 733 days, the values were in the range of 12 – 14 %.

The data thus suggest that the released fraction of iodine is slightly lower than the total fission gas release including the release (FGR_{total}).

In the framework of FIRST-Nuclides, similar samples with Gösgen fuel were leached with a bicarbonate solution under 40 bar Ar/8 % H_2 during 332 days where the IRF (Instant Release Fraction) of the gases were determined and can be compared with the CumFIAP of ^{129}I [14, 33]. The IRF(^{129}I) was 15.7 ± 1.6 % which is higher than the $FGR_{\text{puncturing}}$ alone (8.3 ± 0.9 %) but if the fraction of gases released during the leaching experiment was added, the total amount of gases released is 23.7 ± 1.8 % (puncture test + leaching experiment) and the same conclusion can be drawn as for the Th1 fuel.

Cesium release

Like for iodine, cesium is often correlated to the behavior of Kr and Xe. Electron probe micro analysis (EPMA) measurements of local Cs/Xe ratios suggested that the Cs release was about 60 % of the fission gases [34]. For the Th1 fuel with a $FGR_{\text{puncturing}}$ value of about 14 %, a fractional Cs release of about 9 % is thus calculated. For the Gos fuel, with a significantly lower $FGR_{\text{puncturing}}$ value (about 8 %), the calculated fractional Cs release would correspond to around 5 %. Leaching studies performed in the FIRST-Nuclides project on a variety of SNF samples (including fuels Th1 and Gos) suggested that the actual Cs release was often lower, though [33].

Figure 13 shows the evolution of CumFIAP(^{137}Cs). The amount of ^{137}Cs retained on the walls of the liners is negligible. Therefore the data series represent accurately the cesium released into the solution. For both the Th1 and the Gos fuel, the release rate of cesium is initially fast and decreases with time. The fastest release is observed with the Th1 fuel samples. For this fuel, the CumFIAP(^{137}Cs) values approaches a steady state after 21 days at around 3 ± 1 % in the three experiments (YWCa and bicarbonate solution). This is similar to the fraction released in the bicarbonate solution under weakly oxidizing conditions in FIRST-Nuclides with the same fuel. Thus, the Cs release is apparently affected neither by the reducing conditions imposed in the present tests with hydrogen gas nor affected by the type of leachate.

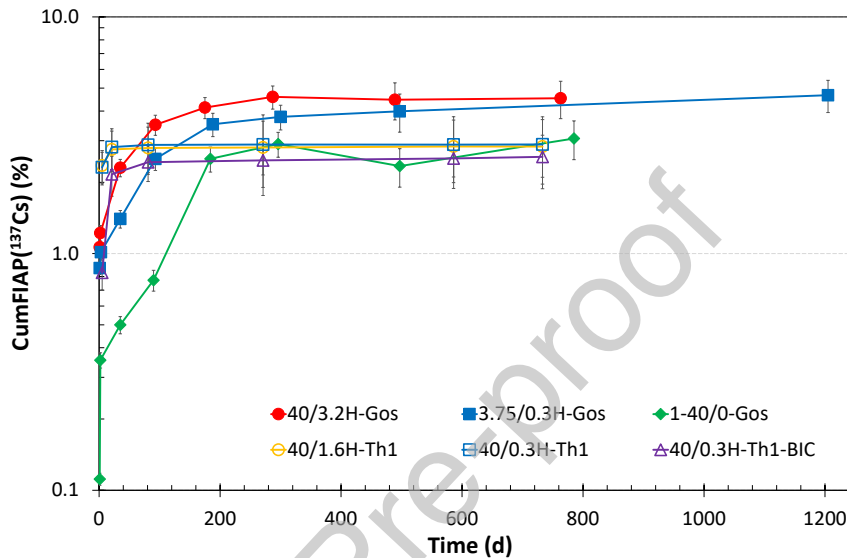


Figure 13: Evolution of the CumFIAP(^{137}Cs) as a function of the time.

For the Gos fuel, it takes longer to approach a steady state level of CumFIAP(^{137}Cs) than for the Th1 fuel, especially in the experiment without hydrogen and low total pressure (1 – 40 / 0 – Gos) where the CumFIAP(^{137}Cs) values also remain lower than in the Gos experiments with H_2 . Furthermore, an effect of the total pressure at the early stage can be observed: at a low total pressure the release of cesium is slower compared to the Cs release in experiments with 40 bar total pressure, but this has no consequences at the end of the experiments. For the experiments under H_2 very similar short-term results ($t_0+5\text{d}$ and $t_0+21\text{d}$) are obtained in the experiment with the Th1 fuel samples performed under 40 bar pressure, while a difference – a delay – in the experiments with the Gos fuel samples under 1 and 3.75 bar can be observed. The total pressure might have an effect on the short-term release of the fraction that is easily accessible to water but not on the cesium fraction released after one year or later, which is presumably included in the spent nuclear fuel matrix; the CumFIAP reached very similar values at the end of two series of experiment (Th1 and Gos fuels). This implies also that Cs is not an appropriate matrix dissolution indicator on the short-term (< 200 days). Although the Cs is initially released slower, CumFIAP(^{137}Cs) values of 4 – 5 % obtained for the longer durations are higher with the Gos fuel than those with the Th1 fuel. These values for the Gos fuel are similar to those found with the same fuel in bicarbonate solution with 3.2 bar H_2 gas pressure and a total pressure of 40 bar [33].

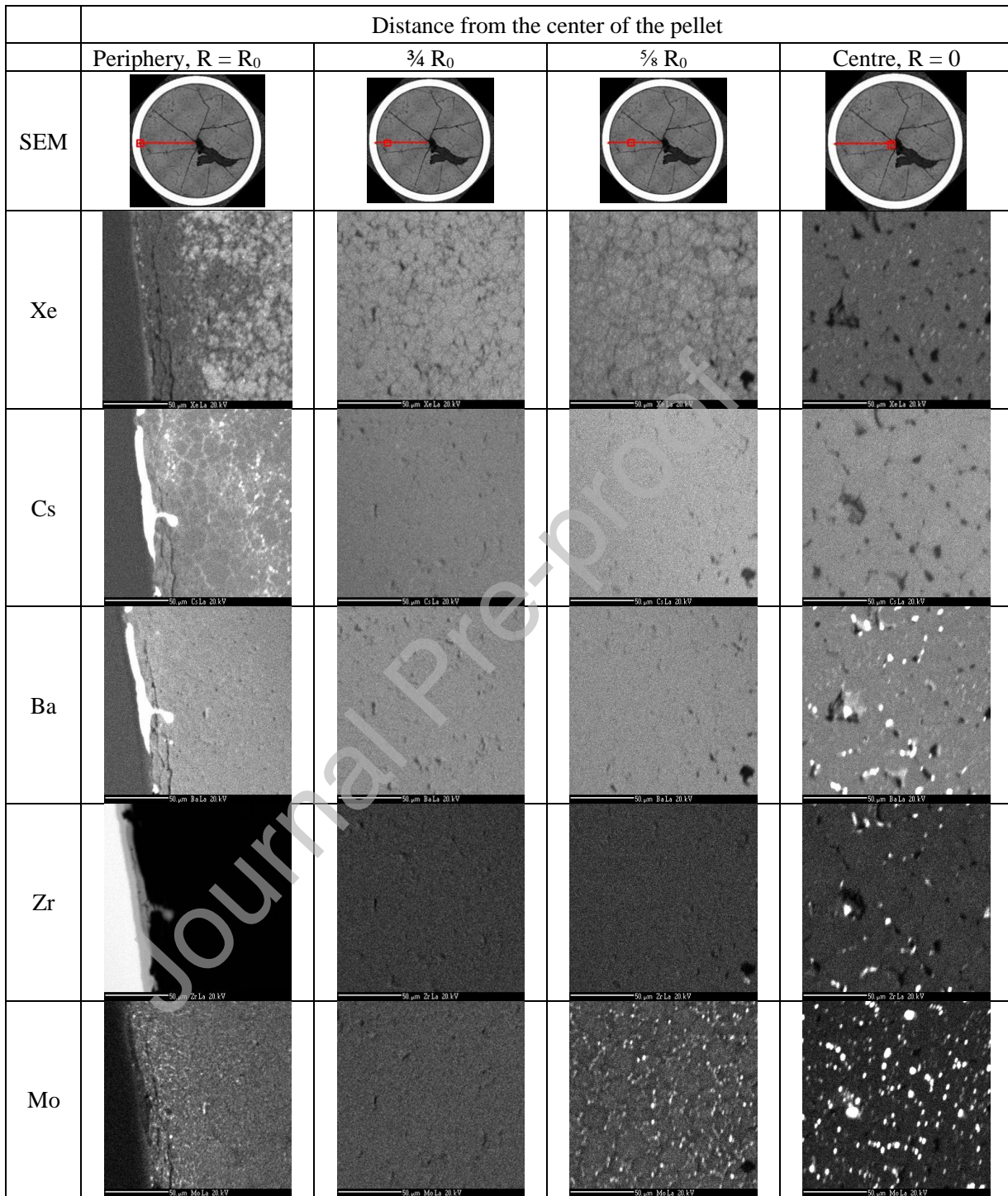


Figure 14: Local mapping of the Tihange 1 fuel sample at different positions for Cs, Ba, Zr and Mo using EPMA. Post irradiation examination of freshly prepared and unleached sample in the framework of FIRST-Nuclides [35].

The Gos fuel thus reaches a higher fractional Cs release, despite the higher burnup and LPR of the Th1 fuel. A possible explanation is that at higher temperatures during the irradiation of the Th1 fuel, the mobility of Cs is more promoted and thus it condensates at colder positions within the fuel rod, as for example at the pellet-clad interface (Figure 14). High Cs concentrations are found in thin layers of Th1 fuel, probably along the UO_2 grain boundaries and at the fuel cladding interface, where a bonding layer is formed inside the inner cladding oxide layer. Similarly, an enrichment of Cs is observed at the pellet-clad interface of the Gos fuel [36]. According to SEM-EDX (Figure 15) analyses, Cl-uranate and complex Cs-U-O-Zr-Cl bearing compounds are formed at the inner ZrO_2 layer of the Gos fuel's cladding. So far, a quantitative comparison of the extent of Cs enrichments at the Th1 pellet-clad interface with that at the Gos pellet-clad interface is not available.

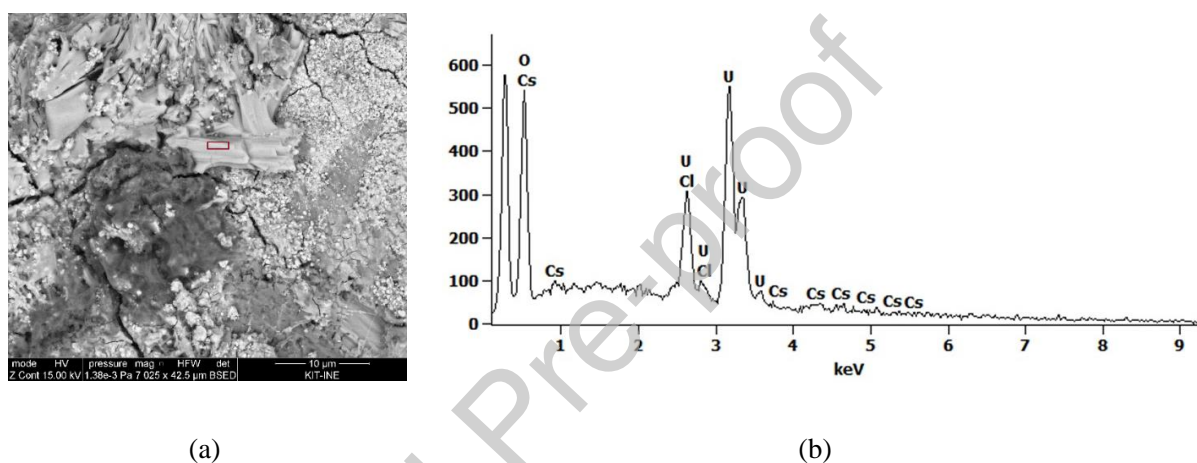


Figure 15: (a) SEM micrograph of crystalline Cs-U precipitates and (b) SEM-EDX spectrum of an exemplary analysis region (marked with a rectangle in the micrograph) at the pellet/cladding interface of Gos fuel.

During leaching, the Cs release is not solubility controlled since the concentrations shown in Figure 6 are far below the solubility limits of expected solid phases, such as cesium chloride ($\log K^\circ = -1.55 \pm 0.01$ for the reaction $\text{Cs}^+ + \text{Cl}^- \leftrightarrow \text{CsCl}_{(\text{cr})}$; [37]).

Strontium release

Whereas the release of Cs approaches a steady state with hardly any further increase of the aqueous Cs concentration, the Sr concentration in solution noticeably continue to increase throughout all experiments with Th1 and Gos fuels, except one outlier in experiment 40 / 3.2H – Gos (Figure 7). It is emphasized that during the experimental duration, no considerable influence of the gas atmosphere on the Sr release is observed.

For the two experiments with the Th1 fuel samples in contact with YCWCa, the different hydrogen concentration does not result in a considerable effect on the Sr concentration (Figure 7) or cumulated fractional Sr release (Figure 16). Similarly, in the experiments with the Gos fuel in YCWCa under either

hydrogen atmosphere or pure argon, Sr concentrations are almost the same within error. In presence of bicarbonate solution, the strontium release showed a different evolution with the Th1 fuel sample and the concentration increased continuously up to $2 \times 10^{-7} \text{ mol.L}^{-1}$. This faster release could be a consequence of a faster dissolution of the UO_2 matrix where Sr is partly dissolved. Sr is not redox sensitive and the dissolution of the UO_2 matrix is known to be promoted by carbonate species. Any differences between two experiments would be related to the sensitivity of the UO_2 matrix, and a different uranium concentration evolution as a function of the leaching time would also be observed under these experimental conditions. However, this statement cannot be verified because of the scattered uranium concentrations as observed in Figure 4-a and the large quantity of uranium sorbed on the vessel walls (Figure 4-b).

The strontium release is not solubility controlled since the concentrations are far below the solubility limits of the expected solid phases, such as strontium carbonate ($\log K^\circ = -9.27 \pm 0.02$ for the reaction $\text{Sr}^{2+} + \text{CO}_3^{2-} \leftrightarrow \text{SrCO}_3$; [37])

For the release of Kr, Xe, I and Cs there are no relevant differences related to the leachate composition and H_2 partial pressure, indicating that the released fractions of these fission products are predominantly situated on the sites that are directly water accessible. In case of ^{90}Sr , the hydrogen pressure can have some minor effects on the CumFIAP but the main difference is attributed to the solution composition (Figure 16). The fractions sorbed on the liners and measured in the rinsing solutions are also plotted. Like for uranium, this fraction was arbitrarily added to the last sampling of each series.

For the Gos fuel experiments, the results are very similar for all tests in YCWCa. CumFIAP(^{90}Sr) is about $5 \times 10^{-4} \%$ at the last sampling, which is lower than the cumulated FIAP of $2.3 \times 10^{-3} \%$ that was obtained with a cladding segment of the same fuel in FIRST-Nuclides after 333 days in a bicarbonate solution and 3 bar H_2 partial pressure (40 bar total; Ar/ H_2 gas mixture) [38]. In case of Th1, the Sr released in solution is also much higher in the bicarbonate medium than in YCWCa, even after including the sorbed fraction, and a cumulated FIAP of $2 \times 10^{-1} \%$ was determined in bicarbonate solution under weakly oxidizing conditions (FIRST-Nuclides) [33, 38].

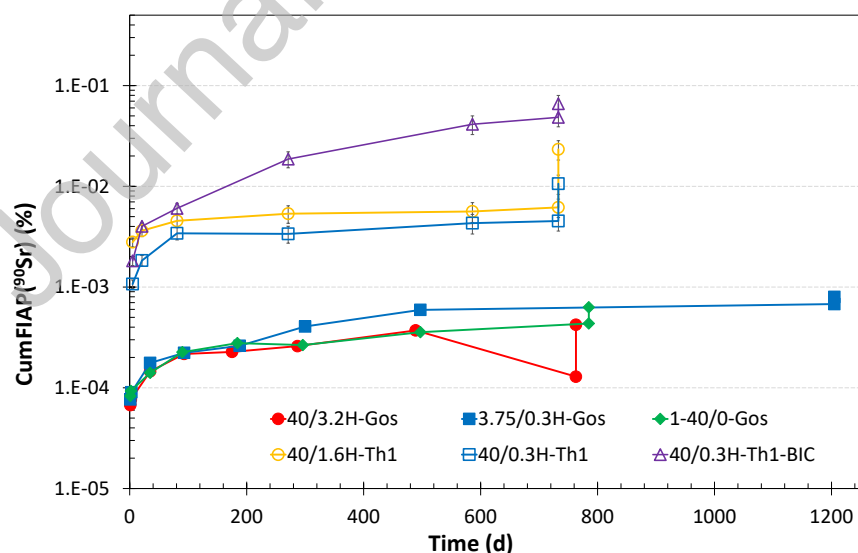


Figure 16: Evolution of the CumFIAP(^{90}Sr) as a function of the time.

For all tests, the Sr release is at least one order of magnitude larger for the Th1 fuel than for the Gos fuel. The higher release of strontium for the Th1 fuel can be related to the fuel properties and, in particular, the

higher LPR in the later irradiation cycles, promoting the formation of Sr-containing ceramic precipitates, which segregated from the UO_2 matrix [39]. Sr was not part of the analyzed elements in [35], but it should exhibit a similar behavior as Ba, which was analyzed. Figure 14 indeed shows a segregation of Cs, Ba and Zr in the periphery of the pellet and the formation of Ba-Zr clusters at the very center of the pellet, promoting the presence of Sr in accessible surface sites [40]. Still, segregation of Ba may be slightly promoted according to the lower solubility of Ba in the UO_2 matrix in comparison to Sr.

The sorption of strontium on the liners was more predominant in the experiments with the Th1 fuel than with the Gos fuel. Likewise, this was observed for the sorption of uranium. Since all liners were made out of titanium and provided by the same manufacturer, their material characteristics cannot explain this strong discrepancy between the two series of experiments. The sole difference between the experimental series was the rinsing duration of the liners: one day in the experiments with the Gos fuel samples and one week with the Th1 fuel samples. Additional measurements were planned at the end of the experimental program with the Th1 fuel in order to scrutinize this difference.

Technetium release

Technetium is redox sensitive and expected to be in the +IV oxidation state in the studied pH range under reducing conditions. The concentrations shown in Figure 8 are significantly lower than the solubility of $\text{TcO}_2(\text{am,hyd})$ of $3.2 \pm 0.3 \times 10^{-6} \text{ mol.L}^{-1}$ determined in previous studies in $0.5 \text{ mol.L}^{-1} \text{ KCl} - \text{KOH}$ solutions and in synthetic cement pore water at pH 13.3 [41, 42]. Most of the aqueous Tc concentrations in experiments with the Gos fuel are lower than those measured in the experiments with the Th1 fuel. However, the Tc concentrations of the Gos fuel display a considerable scatter in comparison to the data of the Th1 experiments. Therefore, a clear distinction between the Tc release from Gos and from Th1 fuel cannot be drawn. In contrast to the dispersion of aqueous U(IV) concentrations, which might be caused by the predominance of the neutral $\text{U}(\text{OH})_4(\text{aq})$ species, a predominance of a neutral Tc species in solution is not likely. In case of technetium, the scatter may be attributed to the relatively low Tc concentrations (even below the solubility of the respective Tc(IV) solid phase). At this concentration range, a dispersion in concentration data is not surprising.

The evolution of the CumFIAP(^{99}Tc) is presented in Figure 17. The first values obtained in the experiment 40 / 3.2H – Gos are not available, which are likely the fractions providing the highest values, therefore they are not shown. The results in pure Ar atmosphere (1 – 40 / 0 – Gos) are quite stable but the concentration increases by five orders of magnitude at the last sampling (Figure 8), which is likely an outlier. In the other four experiments performed in presence of hydrogen, the CumFIAP values are stable over the whole duration, but the hydrogen pressure has little effect. Sorption of technetium on the wall of the liners also occurred, but the sorbed fraction is negligible and only slightly increases the CumFIAP. Like for uranium and strontium, the sorbed fraction was arbitrarily added to the last sampling point, and depicted as a second data set in Figure 17.

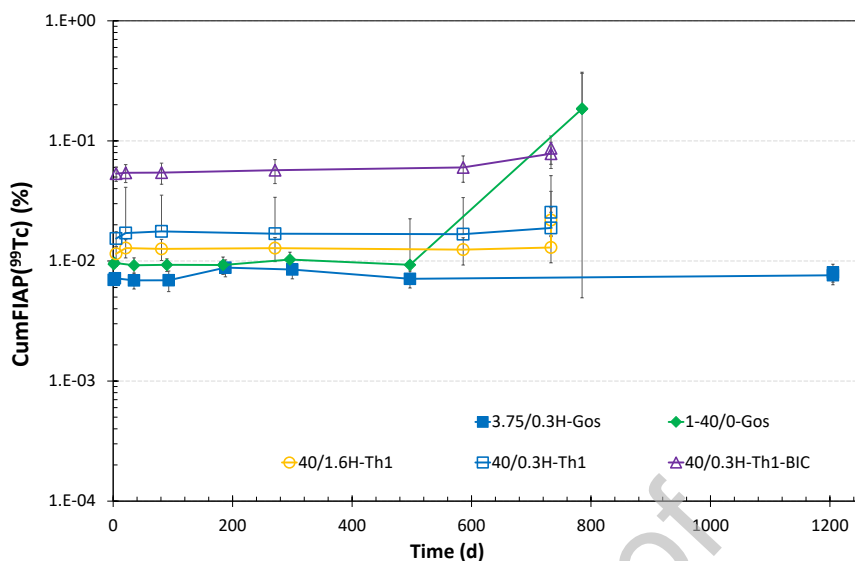


Figure 17: Evolution of the CumFIAP(^{99}Tc) as a function of the time. The second dataset at the end of each series corresponds to the fraction sorbed on the autoclave liners.

If we omit the result at 785 days in the experiment 1 – 40 / 0 – Gos, it appears that the highest results are obtained in the experiment performed with the bicarbonate solution. About 0.08 % of the ^{99}Tc is released from the Th1 spent nuclear fuel after 733 days, including the fraction from the rinsing solution. In an experiment with samples from the same fuel rod, conducted in the carbonated medium under weakly oxidizing conditions, the Tc release of 0.10 ± 0.03 % was reached already after one year [13].

In Figure 17, it is shown that the obtained CumFIAP(^{99}Tc) values in the experiments with the Th1 fuel are slightly higher than those in the experiments with the Gos fuel. As mentioned above, a clear distinction between the Tc release from the Gos and from the Th1 samples is not observed. A hypothetical tendency of higher Tc release from Th1 fuel compared to the release from Gos fuel could be explained by the higher LPR of the Tihange 1 fuel and the higher temperature reached during the irradiation. Although Tc is assumed to be not volatile, its mobility can be affected by the decay chain of Mo. Therefore, it is conceivable, that Tc is present in the more accessible areas of the fuel pellet. This was observed during experiments with the Th1 fuel within the FIRST-Nuclides project where large Mo precipitates were observed from the center of the pellet to the half pellet radius and very small precipitates at the very periphery of the pellet [35].

Accessible Fraction of the Inventory (AFI)

The CumFIAP represents the fraction of the element released in solution, but it does not indicate whether it was released in solution due to the dissolution of the UO_2 matrix or whether this is the result of a fast or preferential leaching of radionuclides present in water accessible structures. To obtain the net preferential release, the (Cumulative) Accessible Fraction of the Inventory (CumAFI) is calculated by subtracting the CumFIAP(^{238}U) from the CumFIAP value at a specific duration, considering the uranium release as an indicator for the matrix dissolution of the SNF [39]. The CumAFI can thus be interpreted as an estimation of the fraction of a radionuclide that is not incorporated in the UO_2 matrix, based on the release in solution measured in leaching experiments. With the exception of iodine, the sorbed fractions are included in the calculation.

Table 6: Cumulative Accessible Fraction of the Inventory, CumAFI (in %), for ^{129}I , ^{137}Cs , ^{90}Sr and ^{99}Tc at the end of the experiments (duration is reported) for the two fuels under the six experimental conditions (values include the sorbed fraction except for ^{129}I).

CumAFI (%)	Gos			Th1		
	40 / 3.2H	3.75 / 0.3H	1 - 40 / 0	40 / 0.3H Bic	40 / 0.3H	40 / 1.6H
Duration (d)	763	1205	785	733	733	733
^{129}I	-	-	-	11.9 ± 5.0	13.0 ± 5.4	13.8 ± 5.0
^{137}Cs	4.5 ± 2.9	4.7 ± 0.7	3.1 ± 0.6	2.8 ± 1.0	2.9 ± 1.7	2.6 ± 0.7
^{90}Sr	$(1.4 \pm 0.9) \times 10^{-5}$	$(4.8 \pm 1.0) \times 10^{-4}$	< 0	$(6.0 \pm 2.1) \times 10^{-3}$	$(3.9 \pm 1.3) \times 10^{-3}$	$(4.6 \pm 1.4) \times 10^{-2}$
^{99}Tc	-	$(7.7 \pm 1.4) \times 10^{-3}$	$(1.8 \pm 1.9) \times 10^{-1}$	$(4.5 \pm 1.7) \times 10^{-3}$	$(1.9 \pm 0.7) \times 10^{-2}$	$(6.7 \pm 2.3) \times 10^{-2}$

The Accessible Fraction of the Inventory is similar to the Instant Release Fraction (IRF) found in the literature, but while the AFI are purely experimental values, IRF values in literature are often estimations of the fast release at the time of the canister breaching. They build further on the knowledge about the AFI of today's fuels, but also involve hypotheses about the further evolution of the fuel. The CumAFI values calculated for the fission products investigated in this study are reported in Table 6. The value for ^{99}Tc in the experiment 40 / 3.2H – Gos is indicated as not available since the missing results for the short durations would lead to an unrealistic CumAFI.

6. Conclusions and perspectives

Leaching experiments were performed with two spent nuclear fuels with a similar burnup but different fabrication process and irradiation histories, in a highly alkaline solution and a bicarbonate solution under anoxic or reducing conditions imposed by the presence of hydrogen, and with durations up to two years or more to investigate the fast release of a selection of fission products. This so-called Phase I of the experiment was followed by a Phase II, not discussed in this paper.

The uranium concentrations of the experiments do not show a consistent evolution, and the cause of the unstable concentrations is not well understood. Consequently, based solely on the uranium releases, no clear effect of hydrogen on the spent nuclear fuel dissolution can be drawn during the first part of the experimental program (Phase I).

At the end of the present experiment, no hydrogen effect was observed on the release of fission gases, as the total amounts of krypton and xenon were similar regardless the fuel samples or the experimental conditions. However, in case of the Gösigen fuel, the ratio Xe/Kr tends to reach the average ratios calculated using the total fuel inventory or the fission gas release determined upon puncturing test, while the ratio Xe/Kr was higher for the Tihange 1 fuel. Moreover, differences have been highlighted on the very short-

term. They were attributed either to the experimental conditions (a higher pressure accelerates the short-term gas release) or to the history of the fuels (opposite evolution of Xe/Kr ratios depending on the fuels).

Considered as volatile and often compared with the fission gas release determined upon puncturing test, iodine was not affected by hydrogen and the CumAFI values in the three experiments with the Tihange 1 fuel were lower than the total fission gas release (puncturing test plus leaching experiment). No clear hydrogen effect was observed on the short-term strontium release and the observed differences were attributed either to the composition of the leaching solution (bicarbonate solution *vs* YCWCa) or to the LPRs. A delay due to the lower total pressure was also observed on the cesium release, implying that cesium is not an appropriate short-term matrix dissolution indicator. At the end of this experimental part and for each fuels, the CumAFI(¹³⁷Cs) were almost identical under YCWCa and under hydrogen, but slightly higher values were determined with the Gösigen fuel than with the Tihange 1 fuel. The hydrogen pressure also had little impact on the technetium release (although it is a redox sensitive element), but the release was higher in the bicarbonate solution.

In the experiments reported in this paper, focusing on the short-term (Phase I), the release of fission products was partly governed by the UO₂ matrix dissolution but much more by the chemical and physical changes in the matrix. These deviations from the reference UO₂ matrix were sensitive to the composition of the leaching solution rather than to the effect of hydrogen. The experimental program has been continued to study the long-term dissolution behavior. A more complete interpretation will be possible once these results are available. Post leaching analyses of the spent nuclear fuels are in preparation. The observations and the measurements will be compared with those performed on freshly cut fuel from the same rod.

7. Acknowledgments

This work was performed as part of the program of the Belgian Agency for Radioactive Waste and Enriched Fissile Materials (NIRAS/ONDRAF) on the geological disposal of high level/long-lived radioactive waste. The authors gratefully acknowledge the technical support from J. Pakarinen, G. Cornelis, B. Gielen, P. Schroeders and G. Cools at SCK CEN, and C. Beiser, E. Bohnert, M. Böttle, M. Fuss, F. Geyer, N. Müller and A. Walschburger at KIT-INE, as well as the workshop staff of both institutes. The SCK CEN group thank also AREVA, Electrabel and Tractebel for the data related to the Belgian fuel rod. The authors would like to thank X. Gaona for providing valuable information on the thermodynamics of actinides and fission products.

8. References

1. Bruno, J. and R.C. Ewing, *Spent nuclear fuel*. Elements, 2006. **2**(6): p. 343-349.
2. Ewing, R.C., *Long-term storage of spent nuclear fuel*. Nature Materials, 2015. **14**: p. 252-257.
3. Metz, V., H. Geckeis, E. González-Roblez, A. Loida, C. Bube, and B. Kienzler, *Radionuclide behaviour in the near-field of a geological repository for spent nuclear fuel*. Radiochimica Acta, 2012. **100**(699-713).
4. ANDRA, *Dossier 2005 Argile, Référentiel de comportement des colis de déchets à haute activité et à vie longue, France*. 2005.
5. IRSN, *PROJET CIGEO - Examen des études remises depuis 2009. TOME 2 - Modèle de relâchement des combustibles usés*. 2013. 2013-00001.
6. Lutze, W. and R.C. Ewing, *Radioactive waste forms for the future*. Vol. chapter 11 (L.H. Johnson and D.W. Shoesmith). 1988.
7. SKB, *Long-term safety for the final repository for spent nuclear fuel at Forsmark*. 2011. SKB, Stockholm, Sweden, TR-11-01
8. Carbol, P., P. Fors, T. Gouder, and K. Spahiu, *Hydrogen suppresses UO₂ corrosion*. Geochimica et Cosmochimica Acta, 2009. **73**(15): p. 4366-4375.
9. Ekeroth, E., M. Granfors, D. Schild, and K. Spahiu, *The effect of temperature and fuel surface area on spent nuclear fuel dissolution kinetics under H₂ atmosphere*. Journal of Nuclear Materials, 2020. **531**: p. 151981.
10. Puranen, A., A. Barreiro, L.Z. Evins, and K. Spahiu, *Spent fuel corrosion and the impact of iron corrosion – The effects of hydrogen generation and formation of iron corrosion products*. Journal of Nuclear Materials, 2020. **542**: p. 152423.
11. Bel, J.J.P., S.M. Wickham, and R.M.F. Gens, *Development of the Supercontainer Design for Deep Geological Disposal of High-Level Heat Emitting Radioactive Waste in Belgium*. MRS Online Proceedings Library, 2006. **932**(1): p. 1221.
12. Wang, L., *Near-field chemistry of a HLW/SF repository in Boom Clay - scoping calculations relevant to the supercontainer design*. SCK ER-17, 2009.
13. Mennecart, T., C. Cachoir, and K. Lemmens, *Fast release from clad and declad spent UOX PWR fuel segments in a bicarbonate solution under anoxic conditions*. Journal of Nuclear Materials, 2021. **557**: p. 153257.
14. Gonzalez-Robles, E., V. Metz, D.H. Wegen, M. Herm, D. Papaioannou, E. Bohnert, G. R., N. Müller, R. Nasyrow, W. de Weerd, T. Wiss, and B. Kienzler, *Determination of fission gas release of spent nuclear fuel in puncturing test and in leaching experiments under anoxic conditions*. Journal of Nuclear Materials, 2016. **479**: p. 67-75.

15. Gonzalez-Robles, E., D. Wegen, E. Bohnert, D. Papaioannou, N. Müller, R. Nasyrow, B. Kienzler, and V. Metz, *Physico-chemical characterization of a spent UO₂ fuel with respect to its stability under final disposal conditions*. Mat. Res. Soc. Symp. Proc., 2014. **1665**: p. 283-289.
16. Kleykamp, H., *The chemical state of LWR high-power rods under irradiation*. Journal of Nuclear Materials, 1979. **84**(1): p. 109-117.
17. Pelowitz, D.B., J.T. Goorley, M.R. James, T.E. Booth, F.B. Brown, J.S. Bull, L.J. Cox, J. Durkee, Joe W. , J.S. Elson, M.L. Fensin, R.A. Forster, J.S. Hendricks, H.G. Hughes, R.C. Johns, B.C. Kiedrowski, R.L. Martz, S.G. Mashnik, G.W. McKinney, R.E. Prael, J.E. Sweezy, L.S. Waters, T.A. Wilcox, and A.J. Zukaitis, *MCNP6 User's Manual*. 2013. LA-CP-13-00634.
18. Wilson, W., S. Cowell, T. England, A. Hayes, and P. Moller, *A Manual for CINDER90 Version 07.4 Codes and Data LA-UR-07-8412*. Los Alamos National Laboratory, 2008.
19. Romojaró, P. and N. Messaoudi, *Inventory calculations for REGAL D05-BU1 sample*. 2022. SCK CEN, R-9197.
20. Iglesias, L., M. Herm, X. Gaona, and V. Metz, *Experimental Investigation of the Radionuclide Release from Spent Nuclear Fuel Samples in High pH Solution under Anoxic / Reducing Atmosphere - Final Report*. 2021. KIT, KIT-INE 001/21.
21. Mennecart, T., *SF-ALE report - Phase I*. 2022. SCK CEN, ER-0759.
22. König, T., *Examination of the radionuclide inventory and chemical interactions on the interface between nuclear fuel and Zircaloy-4 cladding in irradiated LWR-fuel samples*. 2022.
23. Spahiu, K., *Spent Nuclear Fuel Domain 3.1*. EURAD State of Knowledge Report, Version, 2021.
24. Amphos21, *Deliverable D.5.1 - State of the Art report - Update 2013*. 2013.
25. Yu, L. and E. Weetjens, *Estimation of the gas source term for spent fuel, vitrified high-level waste, compacted waste and MOSAIK waste*. 2012. SCK CEN, ER-162.
26. Loida, A., R. Gens, C. Bube, K. Lemmens, C. Cachoir, T. Mennecart, and B. Kienzler, *Corrosion behavior of spent nuclear fuel in high pH solutions – Effect of hydrogen*. Mat. Res. Soc. Symp. Proc., 2012. **1475**: p. 119-124.
27. Loida, A., R. Gens, V. Metz, K. Lemmens, C. Cachoir, T. Mennecart, and B. Kienzler, *Corrosion behavior of High Spent Fuel in Highly Alkaline Solutions*. Mat. Res. Soc. Symp. Proc., 2009. **1193**: p. 597-604.
28. Sjöland, A., P. Christensen, L.Z. Evins, D. Bosbach, L. Duro, I. Farnan, V. Metz, U. Zencker, J. Ruiz-Hervias, N. Rodríguez-Villagra, M. Király, P. Schillebeeckx, D. Rochman, M. Seidl, R. Dagan, M. Verwerft, L.E. Herranz Puebla, D. Hordynskyi, F. Fera, and E. Vlassopoulos, *Spent nuclear fuel management, characterisation, and dissolution behaviour: progress and achievement from SFC and DisCo*. EPJ Nuclear Sci. Technol., 2023. **9**: p. 13.
29. Grambow, B. and K. Lemmens, *Model uncertainty for the mechanism of dissolution of spent fuel in nuclear waste repository*. MICADO European Commission, 2010.
30. Çevirim-Papaioannou, N., E. Yalçıntaş, X. Gaona, K. Dardenne, M. Altmaier, and H. Geckeis, *Redox chemistry of uranium in reducing, dilute to concentrated NaCl solutions*. Applied Geochemistry, 2018. **98**: p. 286-300.
31. Tasi, A., X. Gaona, D. Fellhauer, M. Böttle, J. Rothe, K. Dardenne, D. Schild, M. Grivé, E. Colàs, J. Bruno, K. Källström, M. Altmaier, and H. Geckeis, *Redox behavior and solubility of plutonium under alkaline, reducing conditions*. Radiochimica acta, 2018. **106**(4): p. 259-279.
32. Puranen, A., L.Z. Evins, A. Barreiro, O. Roth, and K. Spahiu, *Very high burnup spent fuel corrosion & leaching under hydrogen conditions*. Journal of Nuclear Materials, 2022: p. 154027.
33. Lemmens, K., E. González-Roblez, B. Kienzler, E. Curti, D. Serrano-Purroy, R. Sureda, A. Martínez-Torrents, O. Roth, E. Slonszki, T. Mennecart, I. Günther-Leopold, and Z. Hózer, *Instant release of fission products in leaching experiments with high burnup nuclear fuels in the framework of the Euratom project FIRST- Nuclides*. Journal of Nuclear Materials, 2017. **484**: p. 307-323.
34. Lassmann, K., A. Schubert, J. Van de Laar, and C. Walker. *On the diffusion coefficient of caesium in UO₂ fuel*. in *Proc. Seminar on Fission Gas Behaviour in Water Reactor Fuels*. 2002.

35. Verwerft, M., B. Vos, S. Van den Berghe, and K. Govers, *First Nuclides: Post-irradiation examination report ROD D05-OM1*. 2014. SCK CEN, R-5579.
36. König, T., M. Herm, A. Walschburger, D. Schild, R. Dagan, J. Rothe, K. Dardenne, T. Prüßmann, V. Metz, and H. Geckeis, *Examination of volatile fission and activation products within the fuel-cladding interface of irradiated PWR fuel rod segments*. 2021, Gesellschaft für Anlagen- und Reaktorsicherheit (GRS): 5th Workshop on the Safety of the Extended Dry Storage of Spent Nuclear Fuel.
37. Giffaut, E., M. Grivé, P. Blanc, V. Philippe, E. Colàs, H. Gailhanou, S. Gaboreau, N. Marty, B. Made, and L. Duro, *Andra thermodynamic database for performance assessment: ThermoChimie*. Applied Geochemistry, 2014. **49**.
38. Amphos21. *IRF Database*. 2012 2012; Available from: <http://www.firstnuclides.eu/>.
39. Cacho, C., *Accessible fraction of the radionuclide inventory of the spent nuclear fuel (AFI)*. 2018. SCK CEN, ER-0407.
40. Govers, K., D. Boulanger, K. Meert, G. Leinders, and V. M., *Characterization of Belgian spent fuels assemblies*. 2019. SCK CEN, BLG-1142.
41. Baumann, A., E. Yalçıntaş, X. Gaona, R. Polly, K. Dardenne, T. Prüßmann, J. Rothe, M. Altmaier, and H. Geckeis, *Thermodynamic description of Tc(IV) solubility and carbonate complexation in alkaline NaHCO₃-Na₂CO₃-NaCl systems*. Dalton Transactions, 2018. **47**(12): p. 4377-4392.
42. Yalçıntaş, E., X. Gaona, M. Altmaier, K. Dardenne, R. Polly, and H. Geckeis, *Thermodynamic description of Tc(IV) solubility and hydrolysis in dilute to concentrated NaCl, MgCl₂ and CaCl₂ solutions*. Dalton Transactions, 2016. **45**(21): p. 8916-8936.

Author statement

T. Mennecart: Conceptualization, Methodology, Validation, Formal Analysis, Investigation, Data curation, Writing – Original Draft, Writing – Review & Editing, Visualization, Supervision, Project administration.

L. Iglesias: Investigation, Data curation, Formal Analysis, Validation, Visualization, Writing (review & editing).

M. Herm Methodology, Investigation, Data curation, Validation, Visualization, Writing (review & editing).

T. König Methodology, Investigation, Data curation, Validation, Visualization, Writing (review & editing).

G. Leinders: Writing (review & editing), Project administration.

C. Cacho: Conceptualization, Writing – Original Draft, Writing – Review & Editing, Supervision

K. Lemmens: Conceptualization , Validation, Writing – Original Draft, Writing – Review & Editing, Supervision, Project Administration.

M. Verwerft: Validation, Writing (review & editing) , Project administration.

V. Metz Methodology, Data curation, Validation, Supervision, Writing (review & editing).

E. González-Robles Conceptualization, Writing (review & editing).

K. Meert: Conceptualization, Validation, Project administration, Funding acquisition.

T. Vandoorne: Conceptualization, Validation, Project administration, Funding acquisition.

R. Gaggiano: Conceptualization, Validation, Project administration, Funding acquisition.

Declaration of interests

The authors declare that they have no known competing financial interests or personal relationships that could have appeared to influence the work reported in this paper.

The authors declare the following financial interests/personal relationships which may be considered as potential competing interests:

Journal Pre-proof